Tewari *et al. Discover Nano* (2026) 21:57
https://doi.org/10.1186/s11671-026-04473-1

Discover Nano

REVIEW

Recent advances in functionalized nanocarbon adsorbents for toxic pollutant removal: challenges and future perspectives

Sanjana Tewari[1], Jasvinder Kaur[1*], Shivanshi Tandon[1] and Dipak Kumar Das[2]

*Correspondence:
Jasvinder Kaur
jasvinderkaur2911@gmail.com
[1]Department of Chemistry, School of Sciences, IFTM University, Moradabad, Uttar Pradesh 244102, India
[2]Department of Chemistry, GLA University, Mathura, Uttar Pradesh 281406, India

Abstract
The increasing release of toxic pollutants into water bodies, especially heavy metal ions (HMs), poses severe environmental and health challenges. Among various remediation techniques, adsorption using functionalized carbon nanomaterials has emerged as an efficient and sustainable approach due to their high surface area, tunable porosity, and diverse surface functionalities. This review systematically evaluates recent advancements in the synthesis, surface functionalization, and adsorption behaviour of carbon-based nanomaterials such as graphene oxide (GO), carbon nanotubes (CNTs), biochar (BC), and activated carbon (AC) for the removal of HMs. Particular attention is given to the roles of oxygen-, nitrogen-, and sulfur-containing functional groups in enhancing adsorption via mechanisms such as electrostatic interactions, ion exchange, surface complexation, redox transformation, and precipitation. The novelty of this review lies in its focused and comparative analysis of how specific surface functional groups influence distinct adsorption mechanisms, capacities, and kinetic/isotherm behaviours across various carbonaceous nanomaterials. Additionally, it highlights recent advancements in multifunctional composite adsorbents such as GO–polymer hybrids, Metal organic frameworks (MOFs)–carbon composites, and metal oxide-functionalized BC that offer synergistic improvements in selectivity, reusability, and stability. By identifying current research gaps and synthesizing recent findings, this review provides a strategic framework for designing next-generation carbon nanomaterials for practical applications in wastewater treatment and environmental remediation.

Keywords Functionalized carbon nanomaterials, Heavy metal ions, Surface functional groups, Adsorption mechanisms, Environmental remediation

1 Introduction

Rapid industrialization and urbanization have significantly contributed to the release of toxic pollutants into water sources, including heavy metals, dyes, pharmaceuticals, and organic contaminants. Although global water demand continues to rise annually, various forms of contamination have severely compromised potential water supplies. Moreover, researchers have warned that climate change impacts, disruptions in the water cycle,

Graphical abstract

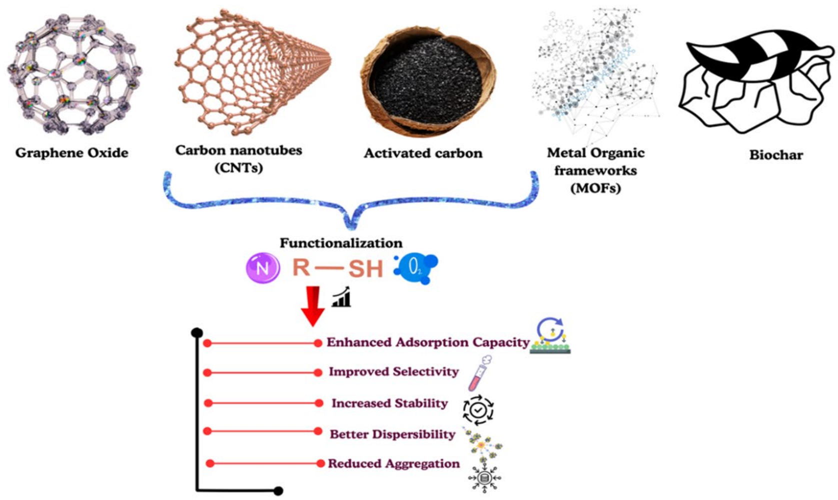

and elevated temperatures will exacerbate water-related challenges, potentially resulting in more frequent droughts and increased toxicity of chemical contaminants due to intensified flooding [1, 2].

Among various water pollutants, potentially toxic metals (PTMs) are particularly concerning due to their non-biodegradability, carcinogenicity, and tendency to bioaccumulate. These heavy metal ions (HMs) are considered among the most severe contaminants, posing serious threats to both aquatic and terrestrial ecosystems [3]. According to the United Nations, nearly 80% of industrial and urban wastewater in developing countries is discharged into the environment without any prior treatment (UN-Water, 2018). In addition, contaminated urban stormwater runoff, agricultural runoff, and rainwater drainage contribute to further pollution of water bodies.

Among all contaminants, HMs are of particular interest due to their toxicity, carcinogenic potential, and well-documented adverse health effects [4]. Over the past several decades, the chemistry, toxicity, and remediation of HMs has been extensively investigated. However, the removal of HMs from water remains a persistent challenge in water treatment. Traditional methods such as membrane filtration, coagulation, electrostatic interaction, chemical precipitation, ion exchange, and adsorption have been widely employed for HMs removal [5, 6]. Nonetheless, these approaches often suffer from drawbacks, including low sensitivity, intrinsic toxicity, and high operational costs. As a result, there is a growing demand for more effective, sensitive, and robust techniques for removing HMs from water samples.

Among these, adsorption stands out as the most economically viable and efficient method for HMs removal. In particular, the use of carbonaceous materials as adsorbents (i.e., carbon adsorbents) has gained significant attention in recent years [7].

Nanotechnology has substantially advanced environmental remediation, especially through the application of functionalized carbon nanomaterials as efficient adsorbents. These materials such as carbon nanotubes (CNTs), graphene oxide (GO), biochar (BC), activated carbon (AC), and metal-organic frameworks (MOFs) possess exceptional properties, including high surface area, tunable porosity, and rich surface chemistry, making them ideal candidates for HMs removal from wastewater. Functionalization further improves their performance by introducing surface groups (e.g., –COOH, –OH, $–NH_2$, C=O), which enhance binding affinity, selectivity, and reactivity toward specific contaminants. These surface modifications facilitate a variety of adsorption mechanisms, including electrostatic interactions, ion exchange, hydrogen bonding, and surface complexation [8].

Recent studies further demonstrate the advantages of functionalized carbon nanomaterials adsorbents. Kumar et al. reported that GO/SiO_2@PANI composites showed enhanced removal of Cr(VI) and Cu(II) due to synergistic effects of polyaniline and silica, which increased both porosity and redox-active sites. In addition to HMs contamination, synthetic dyes constitute another significant class of water pollutants, particularly from textile, paper, and leather industries. These dyes are often carcinogenic, persistent, and resistant to biodegradation, thus requiring effective removal strategies. Interestingly, the same nanocarbon-based adsorbents that are effective for HMs remediation have shown promising performance in removing dyes as well. The adsorption efficiency for dyes is often governed by similar mechanisms—such as electrostatic interactions, π–π stacking, hydrogen bonding, and surface complexation—especially when the adsorbents are functionalized with suitable oxygen, nitrogen, or sulfur groups. Therefore, understanding dye adsorption not only complements the study of heavy metals but also demonstrates the broader applicability of functionalized carbon nanomaterials in wastewater treatment [9]. Similarly, Tanna et al. utilized nano-AC derived from corn cobs to achieve efficient Congo red dye removal, attributed to surface oxygen functionalities and adsorption following Langmuir isotherm behavior. Collectively, these findings highlight how functionalized carbon nanomaterials offer superior adsorption capacity, faster kinetics, higher selectivity, and better regeneration potential—making them promising materials for advanced water treatment applications [10].

With the development of nanotechnology, graphene-based materials such as CNTs, GO, or reduced GO have been extensively researched for their potential utilization in HMs eradication. Graphene consists of a thick sheet of single carbon atoms as hexagonally arrayed sp2 structures has a thickness of 0.334 nm with a 2630 m^2/g surface area [11, 12]. A single-layered GO stands out due to its dense coverage of oxygen-containing functional groups (–COOH, –OH, –C=O), which enhance adsorption through surface complexation and redox interactions. Unlike other carbon materials, GO's sheet-like morphology and π–π stacking capabilities also enable removal of organic and inorganic pollutants [13, 14]. GO has previously been shown to be an active sorbent for several organic contaminant's removal from wastewater, including dyes and antibiotics [15, 16]. Additionally, GO also demonstrated outstanding sorption potential to aqueous HMs ions like Co(II), Cd(II), Au(I), Pb(II), and some radionuclides, such as U(VI) and Eu(III). The sorption progression was mostly organized by the connections between the functional groups of GO surface and the HMs [17–22].

Apart from GO, CNTs have also been extensively explored due to their unique tubular morphology and electronic properties that enhance adsorption mechanisms. Tailored surface functionalization further improves their selective adsorption behavior [23, 24]. The structural features, π-conjugative structures, the curvature of sidewalls, active locations, and morphology are some of the exclusive physical properties of CNTs have allowed augmented adsorptive properties to interact with HMs or atoms through π-π—hydrophobic and electronic interactions [25].

In addition to carbon-based materials like CNTs and GO, MOFs have gained significant attention for wastewater treatment due to their tunable porosity and high metal ion selectivity. As crystalline hybrid structures composed of metal ions and organic linkers, MOFs offer exceptional structural diversity and can be tailored at the molecular level through ligand engineering. This tunability allows for the precise incorporation of functional groups—either during synthesis or via post-synthetic modification—enabling selective adsorption of targeted contaminants. Moreover, the ability to embed dual- or multi-functional moieties within their porous framework facilitates synergistic removal mechanisms, such as simultaneous ion exchange and surface complexation. Reflecting their immense potential, recent literature shows a surge in MOF-based adsorbents for environmental remediation [26]. For instance, Esrafili et al. [27] developed dual-functionalized MOFs (TMU-81) containing sulfonyl and amide groups, which demonstrated high efficiency in removing Cd(II), Cu(II), and Cr(II) from aqueous solutions.

BC, derived from a wide range of lignocellulosic biomass such as wood chips, rice husk, and bamboo, has gained considerable attention as a sustainable adsorbent due to its porous architecture and surface tunability. The nature of the feedstock and pyrolysis temperature significantly influence the physicochemical properties of the resulting BC. To enhance its adsorption performance, BC is often functionalized with metal oxides, alkali metals, or doped with heteroatoms [28]. Recent studies have highlighted the role of engineered BC (e.g., $CaCO_3$-modified BC, magnetite-functionalized BC, and nitrogen- or phosphorus-doped BC) in improving adsorption capacities for Pb(II), Cr(VI), and As(V). Such modifications not only enhance electrostatic interactions and complexation mechanisms but also enable redox transformations in certain cases [29]. For example, $CaCO_3$-modified BC has demonstrated enhanced Pb(II) immobilization via formation of stable carbonates, while Fe_3O_4–BC composites facilitate Cr(VI) reduction and subsequent adsorption as Cr(III) [30, 31]. Hence, the versatility of BC can be significantly improved through controlled pyrolysis and post-synthetic functionalization, making it a viable and cost-effective adsorbent platform [32]. AC surface modification is also useful processes to improve the extraction of metal ions from water with an increment of binding sites for metal ions [33]. Various researches have been performed on the surface chemical properties of carbon for further improvement of their affinity for metal ions. Zhu et al. [34] advocated the application of S and N ligands to the AC surface and improved its adsorption potential against Hg. Liu et al. [35] modified an adsorbent with ethylenediaminetetraacetic acid, which led to the increase carboxyl groups on the adsorbent to lead removal. Yantasee et al. [36] reported amine functionalized AC for adsorption of copper. Likewise, researchers reported that functional groups containing oxygen and nitrogen improve the AC capability to absorb the Cu (II), Cr (VI), Pb(II) metal ions [37–39].

Recently, new 2D carbonaceous materials like graphitic carbon nitride (g-C_3N_4) have gained interest because of their layered nature, rich nitrogen functional groups, and visible-light sensitivity. While more frequently studied for photocatalytic activity, g-C_3N_4 also showed great adsorption capacity toward metal ions and organic dyes upon surface modification or compositing with other materials (e.g., GO, AC, or polymers). The application of g-C_3N_4-based materials in water treatment systems is still in its infancy, but their high content of nitrogen and potential for functionalization render them excellent options for future research [40, 41].

It is widely accepted that the connections between HMs and functional groups of adsorbents lead to a significant contribution to the improved HMs adsorption. Functional groups on carbon surfaces are typically classified according to the heteroatoms they contain, such as oxygen, nitrogen, sulfur, halogens, or phosphorus.Though studies have confirmed that surface modifications of carbon adsorbents significantly improve their properties viz. distribution of pore volume or pore-size, specific surface area, increase in structural constancy, and the amount of functional groups, there is currently a lack of comprehensive data on the surface functional groups interface of carbon adsorbents with HMs [42–45].

With the growing need to treat water pollution and the limitations of traditional remediation methods, carbon nanomaterials have emerged as highly effective adsorbents in the removal of HMs from wastewater. While different reviews have discussed single kinds of carbon adsorbents, including AC, BC, GO, MOFs, and CNTs, and how they are fabricated or their adsorption characteristics, there is still a lack of focused and comparative evaluation that relates particular surface functional groups to the mechanistic functions they perform in adsorbing HMs. This review specifically addresses by systematically examining oxygen-, nitrogen-, and sulfur-containing functional groups included in the carbon nanomaterials architecture and discussing their individual roles in increasing adsorption through mechanisms of electrostatic interaction, surface complexation, ion exchange, redox conversion, and precipitation. In addition, it synthesizes and contrasted recent study outcomes, featuring adsorption capacities, isotherm models, and kinetic behaviors among a broad array of functionalized carbon adsorbents. Moreover, the review highlights recent breakthroughs in multifunctional composite adsorbents, including GO–polymer hybrids, MOFs carbon hybrids, and metal oxide-functionalized BC, that have shown synergistic enhancement in selectivity, stability, and reusability. By highlighting essential research voids and charting future directions, this review thus offers a much-needed roadmap for the rational design of the next-generation carbon-based adsorbents. It therefore provides not just an in-depth knowledge of functional group-specific interactions but also pragmatic information concerning the design of surface chemistry for actual applications in water treatment and environmental remediation.

2 Mechanisms and factors influencing of heavy metal ion adsorption

To provide novel insights, this section links specific adsorption mechanisms with functional groups incorporated onto carbon adsorbents—such as redox interactions facilitated by sulfur containing groups, chelation by nitrogen functionalities, and electrostatic attraction enabled by oxygen-containing moieties. Recent research highlighting the synergistic effects in composite systems and dual-functional adsorbents is also presented, extending beyond traditional adsorption models.

2.1 Fundamental principles governing adsorption

Adsorption is a phenomenon involving the adhesion of molecules or ions (adsorbates) from a gas or liquid onto the surface of a solid substance called an adsorbent [46]. It is distinct from absorption, which involves the penetration of substances into the interior of a material, whereas adsorption is limited to surface-level interactions [47]. Desorption is the reverse process, wherein adsorbed species are removed from the surface [48].

The basic mechanism of adsorption involves mass transport from the bulk fluid phase (gas or liquid) to the solid surface. AC, for example, is engineered with a highly porous structure and a large internal surface area, making it highly effective in capturing organic and inorganic contaminants, including metal ions [49]. The driving force behind adsorption arises from residual surface forces (such as electrostatic or van der Waals forces) present on the adsorbent surface, which are not balanced by the forces in the bulk phase. This imbalance creates surface energy at the interface, thereby attracting adsorbate molecules to the surface [50].

Some of the most important factors determining adsorption include the adsorbent's surface area (a higher surface area allows greater adsorption), pore structure, surface chemistry, and thermodynamic parameters such as adsorption enthalpy and entropy [51]. The efficiency of adsorbents is particularly influenced by these factors. Materials such as AC, BC, MOFs, GO, and CNTs have been reported to exhibit high affinity for pollutants due to their tunable surface properties and porosity [12, 46].

A thorough understanding of the surface functional groups of carbon adsorbents and the interactions between adsorbates and adsorbents is fundamental for designing high-performance materials for water purification. Figure 1 illustrates the key mechanisms governing HMs adsorption at the solid–liquid interface, including electrostatic interactions, surface complexation, ion exchange, and redox transformations.

Carbon adsorbents, their adsorption potential, and associated mechanism for specific metal ions have been presented in Table 1.

2.2 Factors influencing carbon-based adsorption

The adsorption efficiency of carbon-based materials is a function of several interconnected physicochemical properties and external conditions. Among the most critical parameters are surface area and porosity, surface functional group chemistry, particle size and diffusion pathways, and operational factors such as pH, temperature, and contact time. Each of these factors significantly contributes to both the rate and capacity

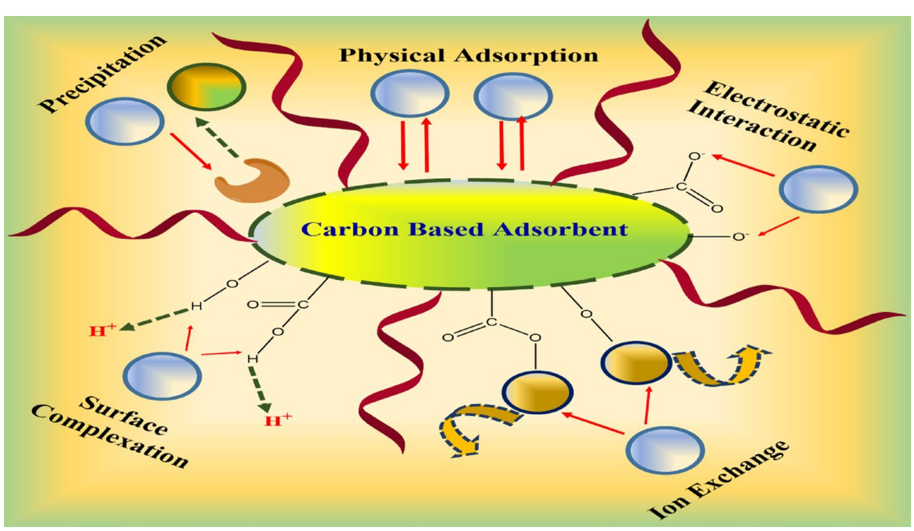

Fig. 1 Schematics adsorption mechanisms for HMs removal

Table 1 Removal of HMs through different carbon-based adsorbents

Carbon based adsorbent	HMs	Mechanism involved	Adsorption capacity (mg/g)	References
GO	Cd(II) As(V)	Chemical adsorption	234 14	[48]
Multi-pore AC obtain from recyclable long-root Eichhornia crassipes	Cu(II) Pb(II) Cd(II) Zn(II) Ni(II)	Electrostatic attraction	277.6 67.9 137.1 56.9 61.9	[49]
GO modified with polyethyleneimine	Pb(II) Cd(II) Hg(II)	Chemical adsorption	374 602 181	[50]
Chitosan/AC/ poly(ethylene-oxide)	Fe(III)	Surface complexation & ion exchange	217.4	[51]
Polyvinylpyrrolidone-reduced GO	Cu(II)	Physical adsorption	1689	[52]
Zerovalent iron decorated functionalized carbon nanotubes	Sb(III) Sb(V)	Chemical adsorption	250	[53]
Cross-linked magnetic chitosan particles	Cu(II) Ni(II)	Chemical adsorption	126.58 66.23	[54]
AC prepared by potato peels	Pb(II)	Physical adsorption	171	[55]
ZnO-Biochar nanocomposite	Pb(II)	Surface adsorption	79.302	[56]
Carbon/Fe-Mn composite	Hg(II)	Chemical adsorption	9.8	[57]
Biochar and humic acid system	Cu(II)	Ion exchange, complexation	35.86	[58]
Multi-walled CNTs modified polyrhodanine	Pb(II)	Chemical adsorption	8118	[59]
Magnetic Zr-MOFs	Pb(II)	Electrostatic attraction	102	[60]
MOFs	Hg(II)	Chemical adsorption	600	[61]

of adsorption by influencing either the thermodynamics or kinetics—or both—of the adsorption process [62].

2.2.1 Surface area and porosity

A high internal surface area is widely regarded as one of the most essential characteristics of efficient carbon adsorbents. This extensive surface area arises from a hierarchically porous structure composed predominantly of micropores (< 2 nm) and mesopores (2–50 nm). Micropores significantly contribute to the overall adsorption capacity by providing a large number of accessible adsorption sites, particularly for small molecules and ions. Conversely, mesopores facilitate faster transport of adsorbate species into the internal regions of the adsorbent, thereby enhancing adsorption kinetics and ensuring that equilibrium is reached in shorter timeframes. Empirical studies have consistently demonstrated that increasing the fraction of micropores leads to higher Brunauer–Emmett–Teller (BET) surface areas, which, in turn, enhances physisorption capacity. Simultaneously, materials with a greater mesoporous volume exhibit improved intraparticle diffusion rates and reduced mass transfer resistance. The pore structure of carbon adsorbents is inherently linked to their method of synthesis [63]. For example, carbonization at high temperatures or graphitization processes typically result in enlarged pore diameters, more ordered graphitic domains, and reduced surface defects. In contrast, low-temperature activation, especially in the presence of activating agents such as H_3PO_4, KOH, or $ZnCl_2$, tends to produce smaller pores and introduce a higher density of oxygen-containing surface groups. The feedstock composition and activation method—whether chemical or physical—not only determine the pore size distribution but also influence pore connectivity, which is vital for efficient mass transfer during adsorption. Thus, by tailoring the activation conditions and precursor characteristics, one can modulate the porosity of carbon materials to optimize both capacity and rate of adsorption [64].

2.2.2 Surface functional chemistry

Surface functional groups play a decisive role in governing the adsorption selectivity and binding mechanisms of carbon-based adsorbents. Typically, these materials possess a range of surface heteroatoms—including oxygen, nitrogen, and sulfur—incorporated as functional groups such as hydroxyl (–OH), carboxyl (–COOH), carbonyl (> C= O), amine (–NH_2), thiol (–SH), and pyridinic nitrogen. These groups can interact with adsorbates through a variety of mechanisms, including hydrogen bonding, π–π interactions, electrostatic attraction, ion exchange, and complexation. For the adsorption of heavy metals and dyes, oxygen-containing functionalities are particularly significant. Carboxyl and hydroxyl groups can act as Lewis bases and form coordination bonds with metal ions, while also influencing the hydrophilicity and charge of the adsorbent surface. At higher pH levels, these groups tend to deprotonate, generating negatively charged sites that favor the uptake of cationic species [7, 65]. Similarly, nitrogen functionalities (e.g., pyridine-like nitrogen or amine groups) may introduce basic sites that are beneficial for binding acidic or anionic pollutants. Chemical modification of the carbon surface can dramatically enhance its functionality and adsorption performance. Acid or base treatments, oxidation (e.g., with HNO_3, $KMnO_4$, or ozone), and heteroatom doping (e.g., N-doping via urea or ammonia treatment) are commonly employed to introduce or augment specific surface groups. Such modifications not only increase the density of active sites but also introduce new adsorption pathways involving chemisorption, ion exchange, or ligand–metal coordination. Functional group density and distribution directly impact adsorption affinity and specificity, and thus are often engineered to match the physicochemical characteristics of target pollutants [66].

2.2.3 External conditions: pH, temperature, and contact time

The ambient conditions under which adsorption occurs—particularly the pH of the solution, temperature, and contact time—can significantly influence both the extent and mechanism of adsorption. Among these, pH is the most crucial, as it affects both the ionization state of adsorbate species and the surface charge of the adsorbent. At low pH, functional groups such as –COOH and –OH remain protonated, leading to a reduction in surface negativity and diminished adsorption of cationic species. As the pH increases, these groups deprotonate, enhancing electrostatic attraction and promoting the binding of metal ions and cationic dyes. However, adsorption capacity may decline at excessively high pH due to precipitation of metal hydroxides, which reduces their availability for surface interaction [67].

Temperature influences adsorption thermodynamics and can either favor or hinder adsorption depending on the dominant mechanism. Physisorption processes are generally exothermic, and thus a rise in temperature typically reduces adsorption capacity. In contrast, endothermic chemisorption mechanisms may become more favorable at higher temperatures, particularly where activation energy barriers exist. Furthermore, adsorption kinetics are affected by temperature, with higher temperatures generally promoting faster diffusion of adsorbates into pores [68].

Contact time is another key variable that governs the equilibrium state of adsorption. The initial rate of adsorption is typically rapid due to the availability of abundant surface sites. Over time, as these sites become occupied and diffusion into microporous regions becomes rate-limiting, the process slows down and approaches equilibrium. Other kinetic parameters, such as initial concentration and the presence of competing ions, also impact adsorption performance and must be carefully optimized for maximum removal efficiency [69].

2.2.4 Particle size and diffusion dynamics

The particle size of carbon adsorbents strongly affects the rate and extent of adsorption, particularly in dynamic systems such as fixed-bed columns or continuous-flow reactors. Smaller particles present a higher external surface area-to-volume ratio and reduce the diffusion path length for adsorbate molecules. This often translates to faster adsorption kinetics and greater apparent capacity. However, extremely fine particles may pose practical challenges, such as elevated pressure drops in filtration systems, poor packing stability, and difficulties in separation and recovery. Therefore, an optimal particle size range is generally selected to balance high performance with ease of operation [70].

In addition, the connectivity of internal pore structures significantly influences diffusion dynamics. Well-interconnected mesoporous networks facilitate the rapid transport of adsorbate molecules from the bulk solution to active sites within the micropores, where the majority of adsorption occurs. Hence, both particle size and internal pore architecture must be engineered in tandem to achieve efficient adsorption [71].

2.3 Influence of surface properties on adsorption efficiency

2.3.1 Electrostatic interaction

Electrostatic forces play an important role in affecting the efficiency of adsorption of HMs onto adsorbents. pH plays an important role in regulating these forces, as it impacts the protonation and deprotonation of the adsorbent surface functional groups. At lower pH levels, protonation of functional groups like carboxyl (–COOH), hydroxyl (–OH), and amine (–NH_2) creates a net positive charge on the adsorbent surface, causing electrostatic repulsion of positively charged HMs, hence decreasing adsorption efficiency. On the other hand, with increasing pH, deprotonation is triggered, which creates a negatively charged surface and increases electrostatic attraction between metal ions and the adsorbent, leading to greater adsorption [72]. The recent literature has emphasized the oxygen-containing functional groups on GO and BC surfaces in electrostatic adsorption processes. The presence of hydroxyl, carboxyl, and epoxy functionalities on GO nanosheets provides efficient electrostatic interaction with Zn(II) for its removal from aqueous solutions. Likewise, gangue microspheres in a geopolymer matrix have a high surface area and rich functional groups (–OH, Si–O–Al, and Si–O–Si), which are responsible for the electrostatic adsorption of HMs [73].

In addition, the surface charge properties of BC are essential in defining its electrostatic adsorption capacity. When the pH of the solution is above the point of zero charge (pHzpc), deprotonation of the surface functional groups of BC leads to the generation of negatively charged sites, promoting electrostatic attraction with cationic metal ions like Cu^{2+} and Zn^{2+}. But below pH pHzpc, protonation results in a positively charged surface, which hinders adsorption efficiency by causing electrostatic repulsion. In addition, the competition between metal ions and H^+ ions for adsorption sites also restricts adsorption at lower pH levels. Some latest studies indicate that surface modification in the form of functionalization by nanomaterials or heteroatom doping can be responsible for boosting the electrostatic adsorption processes. For example, nitrogen-doped carbon materials proved to be a better HMs removing agent due to higher surface charge density and intensified electrostatic interactions. Likewise, addition of metal oxides, e.g., Fe_3O_4 or MnO_2, to carbon-based adsorbents has been shown to greatly enhance electrostatic attraction with metal ions, improving efficiency of adsorption. These observations of electrostatic interactions promise that engineered adsorbents with specially designed surface chemistry can enhance HMs removal in aqueous systems [74].

2.3.2 Physical adsorption mechanism and surface interaction

Physical adsorption, or physisorption, is a phenomenon in which HMs are attached to the surface of carbon absorbents through weak van der Waals forces without creating chemical bonds. The efficiency of adsorption depends mainly on the pore structure, specific surface area, and surface roughness of the adsorbent material, which control the diffusion and entrapment of HMs. Recent research points out that porosity in carbon absorbents is very important for promoting physical adsorption efficiency. High-temperature carbonization has been found to largely enhance the specific surface area and pore volume, thus providing increased adsorption capacity. For example, pine wood BC obtained at 700 °C and grass BC at 300 °C has shown effective Cu(II) and U(VI) removal based on its highly developed porous structure, which improves diffusive surface adsorption [75].

Carbon-based nanomaterials such as GO and CNTs have also been studied due to their capacity for agglomeration in aqueous conditions to produce mesoporous and microporous matrices. Internal surface area increases through these structural characteristics, thus the efficiency of adsorption. The hydrophobicity of CNTs also ensures that metal ions get trapped in the pore network, resulting in higher removal efficiency. Besides, although physical adsorption is largely controlled by porosity and surface area, the latest research suggests that functionalization of the surface can effectively enhance adsorption capacity. Oxygen-containing functional groups like hydroxyl (–OH), carboxyl (–COOH), and carbonyl (–C=O) that are introduced to the surface modify the hydrophilicity of the surface and enhance HMs diffusion into the pore structure. In addition, functionalized carbon materials, including nitrogen-doped BC and metal oxide-impregnated carbon, have shown higher adsorption efficiencies by altering surface interactions while preserving the physical adsorption mechanism.

While physical adsorption is generally thought of as a secondary process for HMs removal, it acts in a synergistic manner with other adsorption phenomena, such as electrostatic interactions, ion exchange, and complexation. As an illustration, a two-mode adsorption system based on microporous AC impregnated with $ZnCl_2$ and KOH was found to make pore diffusion and physisorption both essential in the removal of Ni(II) and Cd(II) from aqueous solutions. Moreover, hierarchically porous materials designed by engineering, like waste biomass-based AC, show improved HMs removal by reconciling micropores for higher surface area and mesopores for greater mass transfer kinetic rates. Nanostructured adsorbents, including MOFs-carbon hybrids and graphene-carbon composites, have also further improved physical adsorption by maximizing pore accessibility and availability of adsorption sites.

Future developments in physical adsorption mechanisms aim at the improvement of adsorbent design by engineered pore size control, surface heteroatom functionalization with nitrogen, sulfur, and phosphorus, and the use of hybrid materials like MOF-carbon and BC-metal oxides. Eco-friendly carbon precursors like agricultural waste-derived BC have also become of interest due to their low cost and environmental advantages in HMs remediation. These new approaches illustrate the emerging function of physical adsorption and the promise of designed adsorbents to enhance the efficiency of adsorption in wastewater treatment processes [76].

2.3.3 Surface complexation and chemical bond formation

Surface complexation plays a crucial role in HMs adsorption, involving the formation of outer- and inner-sphere complexes between metal ions and functional groups on the adsorbent surface. This process is influenced by surface chemistry, pH, and the presence of oxygen-containing functional groups such as hydroxyl (–OH), carboxyl (–COOH), and carbonyl (–C=O). Recent research highlights that GO and other functionalized carbon materials exhibit strong surface complexation capabilities due to their abundant oxygen functional groups, which facilitate stable metal-ligand interactions. For instance, the adsorption of Pb(II) on GO is predominantly governed by surface complexation between Pb(II) ions and oxygenous functional groups, forming stable coordination bonds that enhance adsorption efficiency [77].

The combination of surface complexation and electrostatic attraction has been found to significantly improve HMs adsorption capacity in composite materials. A recent study on anaerobic magnetic granule sludge/chitosan (M-CS-AnGS) composites demonstrated that these materials exhibited enhanced adsorption of Cu(II) and Pb(II) due to the combined effects of complexation and electrostatic interactions [78]. Similarly, CNTs combined with calcium alginate (CA) have shown remarkable performance in HMs removal, particularly at varying pH levels. The Cu(II) adsorption efficiency of CNTs/CA composites increased from 69.9% at pH 2.1 to 83.3% at pH 5.0, suggesting that higher pH enhances surface complexation by facilitating stronger coordination between Cu(II) ions and functional groups. Additionally, the presence of microchannels in CNT-based composites allows for increased ion exchange between Ca^{2+} and HMs, further improving adsorption efficiency [79].

Emerging research has also emphasized the role of BC-based adsorbents in metal complexation. A magnetite-functionalized BC derived from watermelon rinds was recently synthesized as a long-term adsorbent and catalyst for Tl(I) removal from wastewater. Spectroscopic analysis confirmed that Tl(I) adsorption occurred through surface complexation, as evidenced by a decrease in hydroxyl (–OH) groups and an increase in Fe–O bonding after adsorption. These findings suggest that metal–oxygen bonding plays a significant role in the immobilization of metal ions on BC surfaces, making magnetite-based materials effective for long-term HMs removal [80].

The advancement of functionalized carbon materials, metal oxide composites, and hybrid adsorbents has further strengthened the importance of surface complexation in HMs remediation. Recent studies on GO-BC hybrids, CNTs-metal oxide composites, and MOFs have shown that precise surface functionalization enhances metal binding affinity, improving both selectivity and stability in adsorption processes. These modifications allow for greater adaptability across different pH conditions and wastewater compositions, making surface complexation a key mechanism in modern adsorbent design. Future research is expected to focus on tunable surface chemistry, ligand-functionalized adsorbents, and nanostructured materials to optimize chemical bonding interactions for enhanced HMs removal efficiency [81].

2.3.4 Precipitation and crystallization process

Precipitation and crystallization are key processes in HMs immobilization, where metal ions react with counter-ions to create insoluble solids, either on the surface of an adsorbent or within solution. Such processes are instrumental in stabilizing metal pollutants, lowering their mobility in aqueous systems. Current research underscores that metals of intermediate ionization potentials (2.5 to 9.5), e.g., Cu, Zn, Ni, Pb, and rare earth elements, easily precipitate on carbon-based adsorbents and are consequently removed effectively. Precipitation of metal hydroxides, carbonates, sulfides, and phosphates has been determined as a crucial mechanism for the improvement of HMs sequestration. New developments point out that engineered biochars (EBB) from biomass, generated through slow pyrolysis, have greater precipitation potential if they are pretreated with alkaline substances like eggshell waste ($CaCO_3$). It has been proved in studies that Pb(II) adsorption onto $CaCO_3$-modified BC happens largely through precipitation and results in stable mineral phases like $Pb_3(CO_3)_2(OH)_2$ (hydrocerussite) and $PbCO_3$ (cerussite). These results indicate that the adjustment of BC with alkaline precursors is an effective means to enhance its precipitation-driven adsorption efficiency and that it holds great potential for HMs treatment in wastewater remediation [82].

The co-precipitation method has also been investigated in the synthesis of layered double hydroxides (LDHs) with improved crystallization behaviors. Zhang et al. presented a recent work where intercalation of cysteine (Cys) into MgAl-layered double hydroxide (MgAl-Cys-LDH) remarkably enhanced the HMs precipitation through metal-sulfide complexation. The presence of (–SH), ($–NH_2$), and (–COOH) groups in Cys made the stable metal sulfides easy to form, especially for Cu(II), Pb(II), and Cd(II). This alteration not only increased the efficiency of metal removal but also structurally stabilized the adsorbent so that it was not leached under different pH conditions [83]. In addition, nanostructured adsorbents such as GO-based composites and hydroxyapatite-functionalized BC have been explored for their potential to boost precipitation and crystallization processes. These adsorbents offer large surface areas and active sites for metal ion nucleation and crystal growth, thus enhancing sequestration of HMs like arsenic (As), mercury (Hg), and lead (Pb). The combination of Fe/Mn-oxide nanoparticles with carbon-based adsorbents has also been reported to catalyze the crystallization of metal hydroxides, further enhancing the stability of adsorbed metal species [84].

In contrast to conventional adsorption processes dependent significantly on pH-dependent electrostatic forces, precipitation-based adsorption provides increased stability over a wider pH range. According to the latest studies, engineered BC, MOFs, and LDH composites demonstrate negligible changes in performance under different ionic strengths, and thus they are exceptionally effective for real-world wastewater treatment processes. The emphasis of future research is on hybrid precipitation-crystallization processes, wherein multi-functional adsorbents containing phosphate, carbonate, and sulfide groups can selectively adsorb and crystallize HMs into stable mineral phases. These advances are likely to open the door to more efficient, cost-effective, and sustainable technologies in HMs remediation [85].

2.3.5 Ion-exchange and redox reactions

Ion exchange is a common mechanism for HMs removal, whereby metal ions in a solution are swapped with inherent pre-existing cations attached to an insoluble solid matrix in an electro-neutrality sense. Recent studies underscore that carbon absorbents, BC functionalization's, and LDHs are of high ion-exchange capacities as a result of their large amounts of surface-active sites, most notably oxygen-functional groups such as hydroxyl (–OH), carboxyl (–COOH), and phosphate ($-PO_4^{3-}$) groups. This ion exchange process is exceptionally good in removing Cd(II), Pb(II), Cu(II), and Zn(II), with these metal cations displacing alkali and alkaline earth metal cations like K^+, Na^+, Ca^{2+}, and Mg^{2+} from the adsorbent surface [83].

Recent research highlights the function of calcium carbonate ($CaCO_3$)-modified, hydroxyapatite (HAP)-modified, and magnetic nanoparticle-modified engineered BC to improve the ion-exchange process. Hydroxyapatite-derived materials have exhibited remarkable efficacy in sequestering Mn(II), Fe(II), and Pb(II) by undergoing a two-step ion-exchange process. Hydroxyapatite first dissolves at low pH, releasing Ca^{2+} ions and phosphate species, which create a negatively charged surface for metal ion adsorption. Later, Ca^{2+} ions in hydroxyapatite are replaced by metal cations such as Pb^{2+}, Cu^{2+}, and Cd^{2+}, resulting in stable immobilization. Recent advances involving BC-hydroxyapatite nanocomposites have further increased metal retention, even against fluctuations in pH and ionic strength [29, 86].

Aside from ion exchange, redox processes also have an important role to play in the remediation of HMs, especially redox-sensitive metals like Cr(VI), As(III), and Hg(II). Various nanomaterials like nano-zero-valent iron (nZVI), Fe/Mn-oxide-modified BC, and GO-based composites have been designed to provide concomitant adsorption, reduction, and precipitation of harmful metal species. For example, Cr(VI) is reduced efficiently to Cr(III) when it interacts with sulfur-functionalized BC or Fe-nanoparticle composites and cannot be released back into the environment [87]. Analogously, As(III) has been reported to be oxidized to As(V) by MnO_2-modified adsorbents, which is then removed through surface complexation and precipitation [88].

A novel development in ion-exchange-based adsorption is the creation of bio-magnetic membrane capsules (BMMCs) that utilize sodium alginate, polyvinyl alcohol, and magnetic nanoparticles. These capsules remove Cd^{2+} and Pb^{2+} from water effectively using a controlled two-step titration gel crosslinking mechanism, greatly enhancing adsorption capability and material stability. Experiments have also investigated the synergistic action of bimetallic nanoparticles (e.g., Fe-Cu, Fe-Zn) to promote simultaneous ion exchange, redox conversion, and surface complexation, and hence improved multi-metal removal performance [89]. Future developments are centered on hybrid ion-exchange adsorbents, wherein MOFs, carbon nanostructures, and doped metal oxides (TiO_2, Fe_3O_4, MnO_2) are combined to enhance selectivity, regeneration ability, and environmental sustainability. The integration of ion exchange, redox transformation, and co-precipitation mechanisms in one adsorbent system is becoming a very efficient and scale-upable method for industrial wastewater treatment and environmental remediation [90].

3 Functionalization approaches for carbon-based adsorbents

In contrast to prior reviews that summarize surface functionalization methods, this section focuses on how these chemical modifications enhance adsorption selectivity, kinetics, and reusability. We emphasize the interplay between functional group chemistry and performance, including insights from recent innovations in hybrid materials and regenerable adsorbents that are not broadly covered in existing literature. Surface functionalization is crucial for enhancing the performance of carbon-based adsorbents in HMs removal. Introducing specific functional groups modifies the surface chemistry, porosity, and metal affinity of carbon adsorbents. For example, oxidative treatments (H_2O_2, O_3, HNO_3, $KMnO_4$, etc.) graft –COOH, –OH and carbonyl (–C=O) groups onto the carbon surface, increasing its capacity to complex metal ions. Similarly, heteroatom doping has been widely studied: sulfur-containing functionalities (e.g. thiols, sulfides) selectively bind soft heavy metals like Hg(II) and Pb(II), whereas nitrogen-doped carbons (pyridinic-N, amine-N, graphitic-N) favor chelation of metal cations such as Cu(II) and Ni(II) [7]. These modifications illustrate how tailored surface chemistry can dramatically improve adsorption efficiency.

In practice, functionalization strategies span chemical, physical, and biological methods. Chemical approaches (acid/base treatments, oxidation, heteroatom doping) introduce new binding sites; for instance, acid oxidation adds acidic groups, while bases add basic oxygenates. Physical activation (thermal treatment, steam/CO_2 activation, or plasma) can increase surface area and create hierarchical porosity without altering bulk structure. Green or bioinspired routes (using plant extracts, enzymes, or microbial processes) provide eco-friendly alternatives for introducing functional groups. Hybrid composites such as carbon–metal oxide or carbon–MOFs hybrids, or carbon coated with natural polymers (chitosan, tannins) or conductive polymers (polyaniline, polypyrrole) combine multiple adsorption mechanisms and often exhibit improved selectivity, stability, and regenerability [91]. Following applications, functionalization methods, and comparative efficiencies are described below:

3.1 Strategies for enhancing adsorption efficiency

The adsorption efficacy of carbon materials is greatly enhanced by functionalization methods that create active sites for binding, increase surface interactions, and optimize porosity. Such improvement strategies ranging from chemical modification, heteroatom doping, physical activation, to biological or green functionalization have been extensively utilized to enhance HMs removal effectiveness [92–94].

Chemical modification with acids (e.g., HNO_3, H_2SO_4) or bases (e.g., NaOH, KOH) adds oxygen-containing functional groups such as –COOH and –OH onto the adsorbent surface. These groups increase the material's affinity for metal ions by allowing ion exchange and surface complexation reactions. Oxidizing agents such as H_2O_2 and $KMnO_4$ also enhance the reactive surface sites availability, causing an increase in hydrophilicity and binding of metal ions. Another critical technique is heteroatom doping, which introduces atoms like nitrogen, sulfur, phosphorus, or boron into the carbon lattice. The method introduces functional groups such as amines, thiols, and sulfonic acids, which enhance electrostatic attraction and complexation with certain metal ions. For instance, nitrogen doping creates amine groups that bind strongly to cationic metals and sulfur doping introduces thiol and sulfonic acid groups with high affinity for soft metal ions such as Pb^{2+} and Hg^{2+} [95].

Physical activation processes like heat treatment at 600–1000 °C, CO_2 or steam, and plasma surface modification enhance porosity and surface area. These processes form hierarchical structures comprising micropores and mesopores that help in capturing metal ions of different sizes and charges simultaneously [94]. Concurrently, biological and green functionalization processes present eco-friendly alternatives. Methods involving bacteria, enzymes, and plant biomolecules insert bioactive functional groups such as polyphenols and organic acids that aid in immobilization and chelation of HMs [96, 97].

Composite and hybrid adsorbents have, in recent years, picked up pace for their synergistic benefits. These adsorbents involve the combination of carbon substrates with metal oxides, polymers, or MOFs, leading to multifunctional adsorbents with improved performance. Prominent examples include Fe_3O_4–GO nanocomposites, which exhibit enhanced redox activity and magnetic separability, and polymer-functionalized BC that provide enhanced selectivity and mechanical stability [98, 99]. In summary, functional group chemistry is essential to defining the adsorption characteristics of carbon-based materials. By means of optimized surface engineering strategies, one is able to profoundly enhance the stability, selectivity, and capacity of such adsorbents for effective wastewater remediation processes [100].

3.2 Impact of surface modification on selectivity and stability

3.2.1 Oxidation-induced functionalization and surface activation

Surface oxidation is an important modification technique that improves the adsorption performance of carbon-based adsorbents by adding oxygen-functional groups like carboxyl (–COOH), quinonoid, phenol (–OH), lactone, and other acidic functional groups. These functional groups have a great effect on the efficiency of HMs adsorption by enhancing surface interaction and chemical binding affinity. Oxidation is generally performed by exposing carbon adsorbents to strong acids (HNO_3, H_2SO_4/HNO_3, or H_3PO_4), alkalis (NaOH or KOH), ozone (O_3), or oxidants such as H_2O_2, $KMnO_4$, NaClO, and $(NH_4)_2S_2O_8$. All factors like the concentration of oxidants, contact time, and temperature need to be optimized for acquiring desired functionalized surfaces specialized in selective adsorption of HMs. Wet oxidation, however, can cause degradation of structures, which affects the physical integrity of the adsorbent [101]. Figure 2 shows some oxidation treatment processes.

Chemical activation through oxidative treatment (air oxidation or acid oxidation) creates several functional groups (–COOH, –CHO, –OH) on carbon nanotube (CNT) surfaces, increasing the adsorption capacity. These groups also enhance hydrophilicity, making it easier to adsorb low molecular weight pollutants [101]. Metal ion binding is largely through complexation with carboxyl groups, thus enhancing the retention of toxic ions on the surface of the modified CNTs [7]. Moreover, phosphoric acid (H_3PO_4) treatment of BC has been shown to enhance its physicochemical characteristics, resulting in enhanced adsorption efficiency for HMs like Pb(II) and Cr(VI) [102].

GO modification through oxidation incorporates oxygen functional groups (hydroxyl, carboxyl, epoxy), which play a key role in contaminant removal efficiency. Higher oxygen

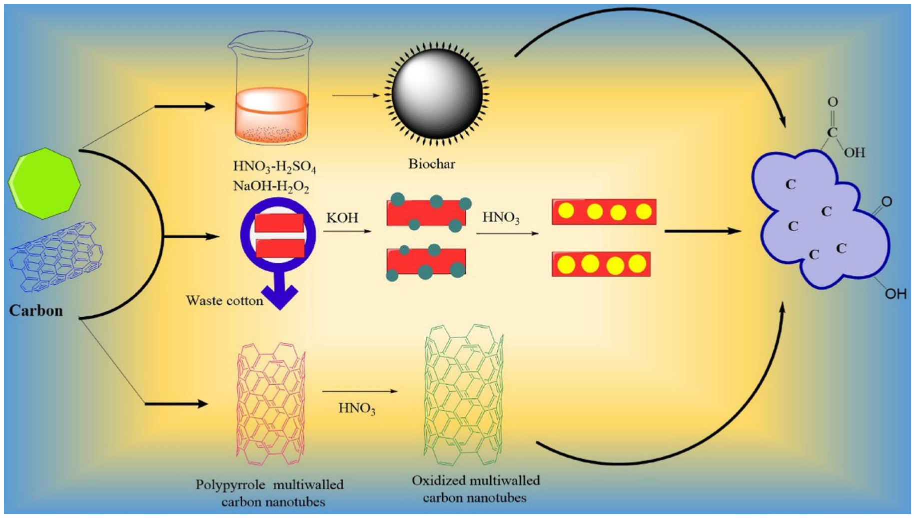

Fig. 2 Routes of synthesis for oxygen-based functional groups

content improves GO's hydrophilicity and solubility, rendering it an excellent choice for biosensors, drug delivery systems, and water treatment. Nonetheless, research on oxygen-controlled synthesis of GO is still limited and needs more investigation to increase its applications in industry [103]. A new MOFs-derived material, porous Fe_2O_3, has been synthesized for high-specific-surface-area adsorption. Pb(II) removal by Fe_2O_3 is through inner-sphere complexation with surface oxygen ions to form covalent bonds that increase adsorption. $Pb(OH)_2$ precipitation under high pH conditions also contributes to HMs removal. The porous Fe_2O_3 synthesized exhibited remarkable adsorption capacity for Cr(VI) (175.5 mg/g) and Pb(II) (97.8 mg/g) and thus serves as a great material for water treatment [104].

Al-Khaldi et al. studied acid-treated carbon adsorbents (CNTs, AC, carbon nanofibers (CNFs), and fly ash (FA)) for the adsorption of Cd(II). The Langmuir isotherm model predicted maximum adsorption capacities of 2.02 mg/g by CNTs, 1.98 mg/g by AC, 1.22 mg/g by CNFs, and 1.58 mg/g by FA. Oxidation significantly enhanced the removal efficiency of CNTs, CNFs, and AC with removal percentages greater than 95%. Nonetheless, oxidized FA showed decreased performance when compared to untreated FA, suggesting oxidation may not be ideal for all types of adsorbents [105]. Another study showed that quinoa crop residue BC that was magnetite nanoparticle-activated and HNO_3-treated showed a remarkable increase in Cr(VI) adsorption capacity. The Freundlich isotherm and pseudo-second-order kinetic models well represented the adsorption process, with modified BC having adsorption capacities of 77.35 mg/g (QBC-MNPs), 55.85 mg/g (QBC-Acid), and 48.85 mg/g (raw QBC). Likewise, oxygen-enriched magnetic BC obtained from K_2FeO_4 synthesis had a remarkable Cr(VI) adsorption capacity of 209.64 mg/g in acidic conditions [106].

Lin et al. prepared oxidized BC from Eichhornia crassipes, where quick adsorption equilibrium was achieved in 30 min and large adsorption capacities for Pb^{2+} (0.57 mmol/g), Cu^{2+} (0.41 mmol/g), Cd^{2+} (0.44 mmol/g), and Zn^{2+} (0.48 mmol/g). The BC preserved its adsorption capability through ten reuse cycles, which shows excellent regeneration performance. Completely, mesoporous carbon which was acid-modified (COMC) demonstrated improved Pb(II) adsorption by greater surface functionalization, whose adsorption complied with the Langmuir isotherm and pseudo-second-order kinetics models [107].

Khandaker et al. investigated oxidized BC for the removal of Cs, where adsorption was found to be best explained by the Langmuir model with a maximum uptake capacity of 55.25 mg/g. Oxidized BC had a high preference for Cs with a removal efficiency of 96% even with co-existing competitive ions like Na and K. The findings indicate that oxidation-created porous structure and oxygen-functional surfaces are primarily responsible for cesium adsorption. In another research, high-energy electron beam irradiation was used to control oxygen content in GO, and controlled oxygenation and improved Pb(II) sorption were attained. Increased doses of irradiation (19.2 kGy) resulted in a Pb(II) adsorption capacity of 636.4 mg/g, affirming the involvement of oxygen-containing functional groups in metal sorption. Also, oxidized multi-walled CNTs(oMWCNTs) modified with polypyrrole (oMWCNT/Ppy) had improved Pb(II) (26.32 mg/g) and Cu(II) (24.39 mg/g) adsorption based on oxygen-functionalized groups (–COOH, –OH, –C=O). The material showed durability through five cycles of regeneration, which made it a potential wastewater treatment material [108].

Tu et al. explored AC produced from Bermuda grass (BGAC) through KOH oxidation. The Langmuir model calculated an adsorption capacity of 403.23 mg/g for Cr(VI), and chemisorption was the prevailing removal mechanism. While encouraging findings, the high acid consumption and operating costs of oxidation treatments are challenges that need to be addressed. Future studies need to work on creating oxidation processes under near-neutral conditions, enhancing HMs recovery, and maximizing large-scale applications to make it economically viable [109].

3.2.2 Nitrogen-enrichment techniques for improved adsorption

Nitrogen-containing functional groups like amino, hydrazine, imine, imidazole, and amidoxime enormously increase adsorption capacity because their lone pair electrons allow for favorable coordination with the pollutant. These functional groups are present both in organic as well as inorganic forms in the form of pyridine-N, graphitic-N, pyrrolic-N, pyridinic-N-oxide, quaternary-N, amine-N, nitrile-N, amide-N, NH_4–N, NO_3–N, and NO_2–N. Of these, quaternary-N and pyridine-N-oxide are more stable than pyrrolic-N and pyridinic-N Fig. 3 shows different nitrogenation treatment techniques [105].

The availability of nitrogen-containing functional groups on the surface of carbon facilitates adsorption through hydrogen bonding and acid/base interactions. Amino-functionalized nitrogen-rich compounds (NA) exhibit great complexation with contaminants. Nitrogen-functionalized GO with nitrogen-containing compounds (NAGO) has generated novel adsorbents with a mix of GO and NA compound properties, which are very efficient for HMs removal from polluted water [110, 111].

Nitration is generally performed with a nitrating medium of concentrated HNO_3 and H_2SO_4 in conditions of reflux. This causes the protonation and dissociation of nitric acid to give nitronium ions (NO_2^+), which are active nitrating agents:

$$\mathrm{HNO_3 + 2H_2SO_4 \rightarrow NO_2^+ + \ H_3O^+ + \ 2H_2SO_4}$$

The reactive NO_2^+ ion allows for electrophilic aromatic substitution on carbon surfaces to give nitroaromatic compounds, which are subsequently reduced by sodium dithionite ($Na_2S_2O_4$). The nitration step is slower compared to the reduction reaction, and

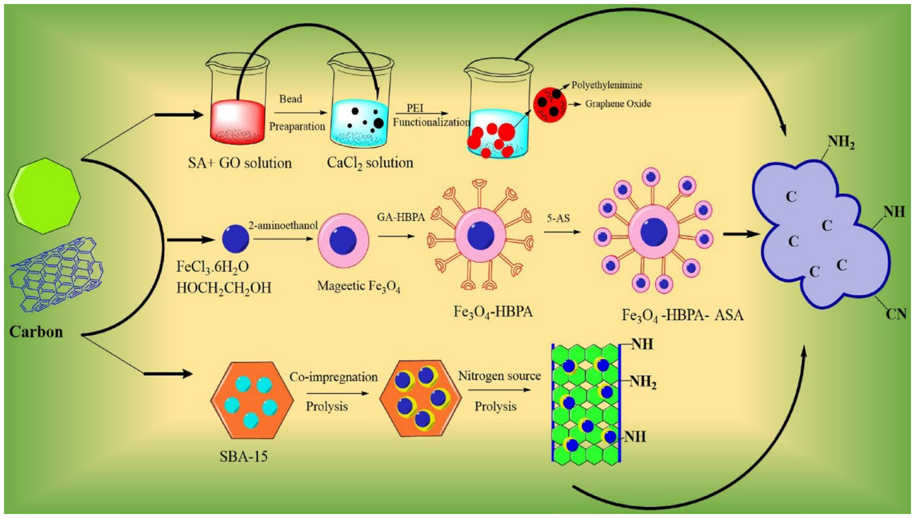

Fig. 3 Routes of synthesis for nitrogen-based functional groups

its yield varies depending on the mixed acid ratio. Raising the ratio from 1:1 to 2:1 or 3:1 decreases reaction time by approximately 30 min. Nonetheless, nitration/reduction treatment can cause pore volume and BET surface area to diminish, although the influence on porous properties is still small. Chelating agents like amino polycarboxylic acids (APCAs) are commonly applied in the stabilization of metal ion complexes. Examples include iminodiacetic acid (IDA), nitrilotriacetic acid (NTA), diethylenetriaminepentaacetic acid (DTPA), and ethylenediaminetetraacetic acid (EDTA). APCAs inhibit metal precipitation, suppress unwanted metal-catalyzed processes, and improve metal ion solubility, thus playing an important role in adsorption operations [112, 113].

Recent research has illustrated the improved HMs adsorption capacities of nitrogen-doped carbon adsorbents. Amino-functionalized $Fe_3O_4@SiO_2$ core-shell magnetic nanomaterials, for instance, successfully adsorbed Pb(II), Cu(II), and Cd(II) ions from polluted water [114]. Nitrogen-doped carbon-MoS_2 (NC-MoS_2) nanohybrid composites had impressive Pb(II) removal efficiency. Polyaniline (PANI) has demonstrated outstanding adsorption affinity for Pb(II) ions [115]. According to Shao et al. [116] With a maximum value of 22.2 mg/g, the PANI/MWCNT magnetic composites demonstrated a markedly increased adsorption capacity for Pb(II) ions. In comparison to unmodified MWCNTs (12.6 mg/g), plasma-treated MWCNTs (13.3 mg/g), and even pure PANI (21.0 mg/g), this performance was noticeably better. The improvement is ascribed to polyaniline's abundant amine and imine functional groups, which bind to Pb(II) ions with great affinity. The composite material's superior adsorption performance is a result of the synergistic effect of PANI modification and the high surface area of MWCNTs. In a similar vein, Yin et al. [117] prepared melamine-modified MOFs for Pb(II) adsorption from low-salt solutions with an adsorption capacity of around 205 mg/g at pH 6. The pseudo-second-order kinetic model fit the adsorption data ($R^2 > 0.99$), establishing coordination interactions between amino groups and Pb(II) ions. Zhang et al. [118] prepared an amino-functionalized MOF (NH_2-MIL-53(Al)) for the selective adsorption of Hg(II) with a maximum capacity of 153.85 mg/g.

Guo et al. investigated the effect of nitrogen doping on BC adsorption capacity. Hydrothermal carbonization of Camellia sinensis at 240 °C (HTC-240) produced BC with highest adsorption capacities for Cu (43.98 mg/g), Pb (83.91 mg/g), and Cr (94.69 mg/g), while BC produced at 280 °C (HTC-280) had greater Zn adsorption (64.78 mg/g). The adsorption processes included metal ion complexation, external mass transfer, and intraparticle diffusion [119].

Chu et al. synthesized a new N-doped bean dregs AC adsorbent (BDC-STM30-10.0HT) to remove Cr(VI). Heat treatment at 1000 °C raised the content of quaternary nitrogen by 18-fold, increasing the adsorption capacity to 3.30 mmol/g under pH 2. The material showed high recyclability with retention of excellent performance in five consecutive regeneration cycles [120]. Geng et al. assessed the adsorption ability of polyethyleneimine-doped GO (GO-PEI) for the removal of Cr(VI). The GO-PEI exhibited a 436.20 mg/g adsorption capacity, which was much greater than that of untreated GO and reduced GO. XPS analysis showed Cr(VI) reduction to Cr(III), and then surface chelation. Electrostatic interactions and redox reactions were involved in the adsorption mechanism, which facilitated chromium ion immobilization [121]. Zheng et al. investigated N-doping modifications of biomass-AC with dicyandiamide through ultrasonic and redox processes. The N-doping treatment enhanced the efficiency of divalent copper ion adsorption considerably. Nonetheless, direct nitrogen impregnation on AC was faced with challenges like extended modification times and low doping efficiency, restricting its influence on adsorption performance. These results point to the success of nitrogen-enrichment processes in promoting carbon-based material adsorption capacities for HMs extraction. Continued studies further optimize nitrogenation processes for increased adsorption efficiency and recyclability towards eco-friendly environmental applications [122].

3.2.3 Sulfuration incorporation for enhanced metal affinity

Sulfuration of adsorbent materials is also possible through reactions with sulfur-containing substances like hydrogen sulfide (H_2S), sulfur dioxide (SO_2), carbon disulfide (CS_2), potassium sulfide (K_2S), phosphorus pentasulfide (P_2S_5), sodium thiosulfate ($Na_2S_2O_3$), elemental sulfur (S_8), and organosulfur compounds by pyrolysis [123]. Physical and chemical properties of adsorbents are affected by the sulfuration process and sulfurizing agents chosen, which might change surface area, porosity, and density of functional groups [28]. Figure 4 shows varied sulfuration treatments.

Due to the high affinity of sulfur functionalities for HMs, sulfur-doped carbon adsorbents have been extensively studied for HMs removal. The incorporation of sulfur functionalities elevates negative surface charges, elevating surface polarity and enabling electrostatic attraction between the adsorbent and positively charged metal cations. Based on Pearson's Hard-Soft Acid-Base (HSAB) theory, soft acid-soft base interactions are responsible for the high affinity of HMs (soft acids) for sulfur functionalities (soft bases) [124].

Among the diverse sulfur functionalities, thiol (-SH) groups have high affinity for other HMs via Lewis acid-base interactions. Representative thiol-based functionalization reagents are mercaptopropyl trimethoxysilane, mercaptobenzimidazole, and dithiocarbamate, which enhance selectivity and adsorption efficiency, particularly for Hg(II) ions. Other sulfur species such as carbon disulfide (CS_2), elemental sulfur (S_8), and hydrogen sulfide (H_2S) are loaded in adsorbents using impregnation methods. This modification has been used in AC, CNTs, and GO [7].

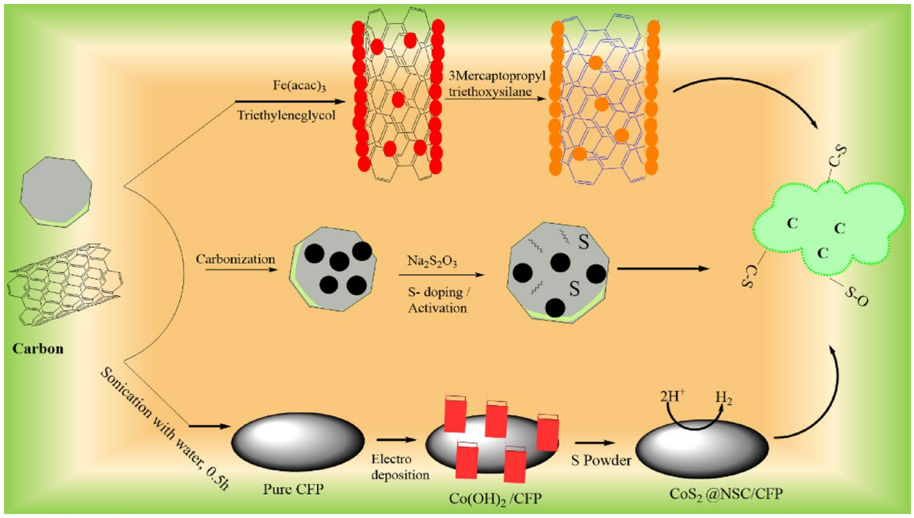

Fig. 4 Distinctive sulfuration synthesis routes into carbon adsorbents

For example, Liu et al. grafting 3-mercaptopropyltriethoxysilane (MPTS) onto CNTs/Fe_3O_4 nanocomposites was accomplished successfully. Enhanced surface area and superparamagnetism were present in thiol-functionalized CNTs/Fe_3O_4 nanocomposites. The adsorption of Hg^{2+} and Pb^{2+} took place according to a pseudo-first-order kinetic model with maximum adsorption capacities of 65.52 mg/g and 65.40 mg/g, respectively [125]. Likewise, Lu and Guo in another work illustrated that Pb(II) ions were removed efficaciously by walnut shell-based sulfur-functionalized adsorbents through ion exchange and complexation, which was best explained by the Temkin adsorption isotherm model. The pseudo-second-order kinetic model best explained the adsorption process, reflecting a chemisorption-dominated mechanism [126].

Wu et al. explored the thiol-functionalization of cellulosic biomass materials, such as absorbent cotton, wood sawdust, and buckwheat hulls, to enhance Pb(II) removal. Thiol-modified absorbent cotton showed a threefold increase in adsorption capacity (28.67 mg/g) compared to unmodified cotton (10.78 mg/g). Wood sawdust and buckwheat hull exhibited increased Pb(II) uptake (43.14 mg/g and 44.84 mg/g, respectively) due to additional metal-binding functional groups [127].

Das et al. investigated xanthate-functionalized Aspergillus versicolor mycelia for cadmium sulfide (CdS) nanoparticle synthesis and Cd^{2+} removal. Palygorskite functionalized with mercapto groups exhibited enhanced adsorption selectivity for Pb^{2+}, Cd^{2+}, and Cu^{2+}. A ligand, 2-hydroxyacetophenone-4 N-pyrrolidine thiosemicarbazone (HAPT), was synthesized and applied for Hg(II) removal, forming stable $[Hg\text{-}HAPT]^{n+}$ complexes with distinct colorimetric changes observable by the naked eye [128].

Fayazi et al. synthesized sulfur-coated magnetic multiwalled CNTs (S-M-MWCNTs) via a heating process, achieving a maximum Hg(II) adsorption capacity of 62.11 mg/g at pH 4.5. Adsorption followed a monolayer chemical adsorption model, with an endothermic and spontaneous nature. Hadavifar et al. further demonstrated that thiol-functionalized MWCNTs had an adsorption capacity of 84.66 mg/g for Hg(II), following Langmuir isotherm behavior. Regeneration studies revealed only a 7.2% loss in adsorption efficiency after five cycles, indicating excellent reusability for wastewater treatment [129].

Despite the promising adsorption capabilities of thiol-functionalized materials, their large-scale industrial application remains challenging due to high synthesis costs. For instance, bulk purchasing of high-purity cysteine (100%) costs approximately \$10–30 per kilogram, while 5-mercapto-1 H-tetrazole-1-acetic acid (99% purity) costs \$10–50 per kilogram. Thus, the upscaling of thiol-functionalized adsorbents may incur substantial production costs, necessitating the development of cost-effective functionalization techniques [130].

4 Role of functional groups in metal ion adsorption

4.1 Contribution of functional groups to binding mechanisms

Functional groups on carbon-based adsorbents are crucial in the adsorption of HMs from water. These functional groups, including oxygen-, nitrogen-, and sulfur-containing moieties, increase the interaction between the adsorbent surface and metal ions, hence enhancing adsorption efficiency. Adsorption is normally assessed by adsorption isotherms and kinetics. The pseudo-second-order model is commonly used to investigate adsorption kinetics and mechanisms of chemisorption. In the analysis of isotherms, the Langmuir model can be used for the calculation of monolayer adsorption capacity, whereas Freundlich model quantifies adsorption intensity and surface heterogeneity [7]. Tables 2, 3 and 4 show the different carbon-based adsorbents functionalized by oxygen, sulfur, and nitrogen groups, and their respective efficiencies in adsorption for different HMs .

4.2 Comparative analysis of various functionalized carbon materials

4.2.1 Oxygen-based functional groups

Oxidation is an impressive technique to increase the efficiency of carbon adsorbents for metal ions removal [131]. The interface between surface oxygen groups and metal ions facilitates HMs adsorption on carbon-based nanomaterials. The effect of oxygen-bearing functional groups on HMs removal by carbon-based adsorbents with their maximal adsorption capability, isotherm, and kinetic models is presented in Table 2. The most common functional group i.e., carboxyl groups and hydroxyl, shows good affinity towards HMs removal of Pb(II), Hg(II), Cr(VI), Cd(II), and Ni (II). The bare CNTs usually involve oxidation or treatments of acid to enhance their surface oxygen-based functional groups, whereas these kinds of treatments are not necessary for graphene since the synthesized graphene material owns an ample amount of oxygen-bearing functional groups [131]. However, if the GO surface gets exposed to additional oxygen-bearing functional groups, its sorption capacity increases further [132].

Fan et al. reported that the adsorption capacity of BC significantly increased after treatment with HNO_3–H_2SO_4 and NaOH–H_2O_2 systems, attributed to the activation of oxygen-containing functional groups, which enhanced cadmium uptake. Adsorption kinetics were analyzed using pseudo-first-order and pseudo-second-order models, while Langmuir and Freundlich isotherms were applied to evaluate the effect of initial Cd^{2+} concentration [151]. Lu et al. proposed a hydrothermal method to modify Fe-based MOF MIL-101(Fe) with GO as shown in Fig. 5, forming a typical sandwich structure, improving the materials water stability and adsorption capacity. As a result of the large specific surface area and abundance of active sites, MIL-101(Fe)/GO exhibited a high adsorption capacity of 128.6 mg/g and an efficient adsorption rate within 15 min, for the

Table 2 Carbon-based adsorbents with oxygen-containing functional groups for the removal of HMs

Absorbent	HMs	Functional groups	Adsorption capacity (mg/g)	Isotherm	Kinetic model	References
GO	Pb(II)	C=O OH C–O COOH	636.4	Langmuir	Pseudo-second-order	[133]
Waste newspaper modified GO	Pb(II) Ni(II) Cd(II)	C–O–C OH C=O	75.41 29.04 31.35	Langmuir, Freundlich	Pseudo-second-order	[134]
MOF	Hg(II) Cd(II) Pb(II)	OH	431 393 397	Langmuir	Pseudo-second-order	[135]
Banana stem char (BN char)	Pb(II)	OH COOH C–O	252.46	Langmuir	Pseudo-second-order	[136]
L-Tryptophan functionalized GO	Pb(II) Cu(II)	OH COOH C–O C=O	222 588	Langmuir	Pseudo-second-order	[137]
Xanthation of Fe_3O_4-chitosan grafted onto GO	Cu(II)	OH C–O C=O	426.8	Langmuir	Pseudo-second-order	[138]
Rape straw BC derived from modified material	Cd(II)	C=O C–O OH	81.10	Langmuir	Pseudo-second-order	[139]
Three-dimensional graphene foam	As(V)	C–O	177.6	–	–	[140]
HNO_3 modified BC	U(VI)	C–O C=O COO	355.6	Langmuir	Pseudo-second-order	[141]
Olive stones AC modified with (HNO_3), olive stones AC modified with (O_3)	Cu(II) Ni(II)	C–O OH	34.163 17.907	Langmuir	–	[142]
BC pyrolytically produced from municipal solid wastes	As(V)	OH C=O O–C	24.49	Langmuir	Pseudo-second-order	[143]
Cymbopogon Schoenanthus L. Spreng modified with H_2O_2	Cu (II)	C=O–OR C=O C–O–C OH C=O	53.8	Langmuir	–	[144]
HNO_3 modified bamboo-derived BC	Cd(II)	OH	44.54	Freundlich	Pseudo-second-order	[145]
AC made from rice straw in presence of H_3PO_4	Hg (II)	OH C–O–C C–O	500	Freundlich	Pseudo-second-order	[146]
Polyethyleneimine (PEI) and GO	Cr(VI)	C=O COOH C–O–C OH	539.53	Langmuir	Pseudo-second-order	[147]
Carbon spheres Oxidized CNTs GO	Pb(II)	C=O OH C–O	250 357 500	Langmuir	Pseudo-second-order	[148]
Acidified multiwalled carbon nanotubes	Pb(II)	COO	93	Freundlich	–	[149]
3D MnO_2nanotubes@reduced GO	Pb(II)	C–O–C C–O C–OH	356.37	Langmuir	Pseudo-second-order	[150]

Table 3 Carbon-based adsorbents with nitrogen-containing functional groups for the removal of HMs

Absorbent	HMs	Functional groups	Adsorption capacity (mg/g)	Isotherm	Kinetic model	References
Polyethylenimine modified GO	Pb (II)	$-NH_2$	602	Langmuir	Pseudo-second-order	[157]
Amino-functional large-size mesoporous silica spheres	Pb(II)	$-NH_2$	48.7	Langmuir	Pseudo-second-order	[158]
Amino-functionalized carbon nanotube through green synthesis and graphene hybrid aerogels	Cu(II) Pb(II)	C=N N–H $-NH_2$	318.47 350.87	Langmuir	Pseudo-second-order	[159]
Tetrazole-bonded bagasse	Pb(II) Cd(II) Cu(II) Ni(II)	C≡N N=N C=N N–N	253.5 196.8 132.5 89.3	Langmuir	Pseudo-second-order	[160]
Amide-functionalized cellulose-based adsorbents	Cu(II)	N–H	51.3	Langmuir	Pseudo-second-order	[161]
Ethylenediamine functionalized multiwall CNTs coated with iron(III) oxide	As(V)	–	23.47	Freundlich	pseudo-second-order	[162]
Urea phosphate (UP) is an activating agent for preparing carbon sorbents derived from biomass	Cd(II)	C–N N–H	40.65	Langmuir	Pseudo-second-order	[163]
Nitrogen-functionalized magnetic ordered mesoporous carbon (N-Fe/OMC)	Pb(II)	C≡N C–N N–H	185.51	Langmuir	Pseudo second-order	[164]
Modification Of multiwalled CNTs through Nitrogen	Pb(II) Zn(II)	C=N C–N	36.23 32.60	Langmuir	Pseudo second-order	[165]
Nitrogen-functionalized carbon nanotubes	Cu(II)	C=N C–N	31.65	Langmuir	Pseudo-second-order	[166]
Nitrogen-functionalized GO	Cu(II)	$-NH_2$, –NH, O–N, O=C–N	34.4	Freundlich	pseudo-first-order	[167]
Nitrogen-doped AC (AC5-600)	Cr (VI)	N-containing groups (amines, pyridinic, pyrrolic)	318	Freundlich	Pseudo-second-order	[168]
Nitrogen-doped porous carbon from biomass	Cr (VI)	C–N	385.8	Langmuir	Pseudo-second-order	[169]
Nitrogen-doped magnetic BC	Cr (VI)	> C=N, –C=N NH	142.86	Langmuir	Pseudo second-order	[170]
Mussel inspired preparation of amine-functionalized Kaolin	Cu(II)	$-NH_2$	20.54	Langmuir	Pseudo-first-order	[171]
Modified UiO-66-NH_2	Cd(II) Cr(III) Pb(II) Hg(II)	N=C=S, N=C=O	49 117 232 769	Langmuir	–	[172]
Nitrogen-functionalized bone chars	Cr(VI) U(VI)	–C=N	339.8 466.5	–	Pseudo second-order	[173]

Table 4 Carbon-based adsorbents with sulfur-containing functional groups for the removal of HMs

Absorbent	HMs	Functional groups	Adsorption capacity mg/g	Isotherm	Kinetic model	References
Sulfurized wood BC	Hg(II)	C–SOx–C	107.5	Langmuir	Pseudo-second-order	[184]
3-mercaptopropyltriethoxysilane (MPTS) was functionalized on the surface of CNTs/Fe_3O_4 nanocomposites	Hg(II) Pb(II)	Si–C	65.52 65.40	Langmuir	Pseudo-second-order	[185]
Mercapto modified magnetic Zr-MOF	Hg(II)	O–Si–O	282	Langmuir	Pseudo-second-order	[186]
Sulfur- a modified metal-organic framework	Hg(II)	NCS^-	439.8	–	Pseudo-second-order	[187]
Sulfur-functionalized silica materials	Hg(II)	–Si–O–Si–	47.50	–	–	[188]
Sulfur-Functionalized Silica Microspheres	Hg(II)	–Si–O–Si–Si–O	62.3	Langmuir	Pseudo-second-order	[189]
Sulfur- modified rice husk	Cd(II)	C–S C=S	137.16	Langmuir	Pseudo-second-order	[190]
Sulfur-functionalized silica	Cd(II) Pb(II)	Si–O–Si Si–O	22.3 46.3	Langmuir	Pseudo-second-order	[191]
Hydroxy sulfate@metal-organicfram	Hg(II)	Cu–S	627.6	Langmuir	Pseudo-second-order	[192]
Sulfur-functionalized sawdust biochar	Cd(II)	C=S C–S S–H SO_3^{2-}	39.38	Langmuir	Pseudo-second-order	[193]
Thiol (SH) and dithiocarbamate (DTC) ligands functionalized with multi-walled carbon nanotubes	Hg(II)	C–S	191.52 57.87	Langmuir	Pseudo-second-order	[194]
Sulfur-modified digestate-derived biochar	Cr(VI)	C–S	52.6	Langmuir	Pseudo-second-order	[195]
Thiol-modified biochar	Hg(II)	–SH C–S–C	118.4	Langmuir	Pseudo-second-order	[196]
Porous puffed rice carbon (PRC) with co-implanted metal iron and sulfur forming high-quality PRC/Fe@S	Hg(II)	S-C	738	Langmuir	Pseudo-second-order	[197]
Sulfhydryl functionalized AC	Pb(II)	S–H	116.3	Langmuir	Pseudo-second-order	[198]
Thiol functionalized MOFs (SH-MiL-68(In))	Hg(II)	S–H	450	Langmuir	Pseudo-second-order	[199]
MIL88A-SH	Hg(II)	S–H C=S	1111.1	Langmuir	Pseudo-second-order	[200]
Sulfur-functionalized magnetic amidelinked organic polymers	Hg(II)	C=S	512	Langmuir	Pseudo-second-order	[201]

Table 4 (continued)

Absorbent	HMs	Functional groups	Adsorption capacity mg/g	Isotherm	Kinetic model	References
Sulfur modified marine brown algae *Cystoseiraindica*	La(III) Ce(III)	C–S S–OR C=S	185.44 172.33	Freundlich	Double–exponential	[202]
Thiol-modified magnetic covalent organic frameworks (M-COF-SH)	Hg(II)	R–S–S–R	383	Langmuir	Pseudo-second-order	[203]

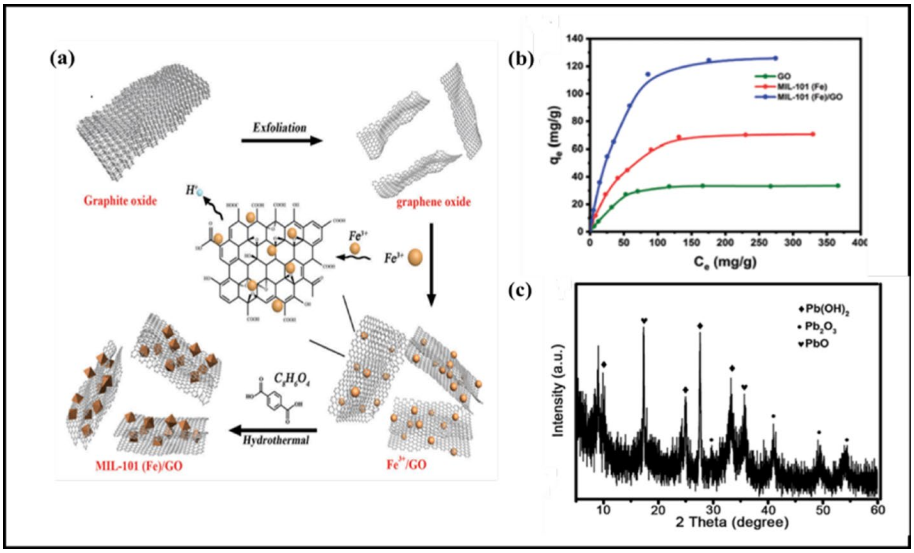

Fig. 5 **a** Schematic illustration of the synthesis of MIL-101(Fe)/GO with a sandwich structure via a hydrothermal method; **b** Pb^{2+} adsorption isotherms for GO, MIL-101(Fe) and MIL-101(Fe)/GO at room temperature; **c** XRD pattern of MIL-101(Fe)/GO after Pb^{2+} adsorption [152].

removal of Pb^{2+} from aqueous solution. The XRD patterns of MIL-101(Fe)/GO before and after Pb^{2+} adsorption revealed a basic adsorption mechanism of ion exchange, in which Pb^{2+} is transformed into oxides and hydroxides via bonding with the oxygen or hydroxy groups of MIL-101(Fe)/GO, respectively [152].

Mashhadimoslem et al. investigated oxygen adsorption on oxidized porous carbon (W-1000-O), with results shown in Fig. 6. The adsorption isotherm revealed that the Sips model best described O_2 uptake, indicating heterogeneous multilayer adsorption. The kinetic data (Fig. 6c) followed the fractional-order model, suggesting a mixed physisorption-chemisorption mechanism. Despite a reduced surface area due to oxidation, the presence of oxygen-containing functional groups (–OH, C=O) significantly enhanced O_2 adsorption capacity (4.11 mmol/g at 298 K, 6 bar), making W-1000-O a highly efficient and selective adsorbent for O_2 over N_2 [153]. Similarly, to oxidize BC, various physical and chemical modification methods were used from several bare materials, and the modification dramatically increased the number of surface oxygen functional groups and rates towards Cd(II), and Pb(II) removal [154–155].

4.2.2 Nitrogen-based functional groups: amine, pyridine, and pyrrole

Nitrogen-doped carbons are versatile materials owing to their unique properties such as outstanding chemical stability, low cost, extraordinary surface area, etc. Especially, it was considered that the heteroatom dopants progress the adsorbents activity via density improvement of a negative charge, the basicity, and wettability functionalities of carbon surfaces. This marked change is attributed to the increased total electron density by N-atom doping, which in turn ameliorates the specific electronic features and adsorbents' ability for adsorption for HMs removal. Table 3 summarizes the studies related to adsorption of HMs by carbon materials bearing nitrogen functional groups and their relative capacity of adsorption and isotherm models and the best-fit kinetics. Onto carbon nanomaterials, the functional groups of nitrogen ($-NH_2$ and –NH) mostly contribute to

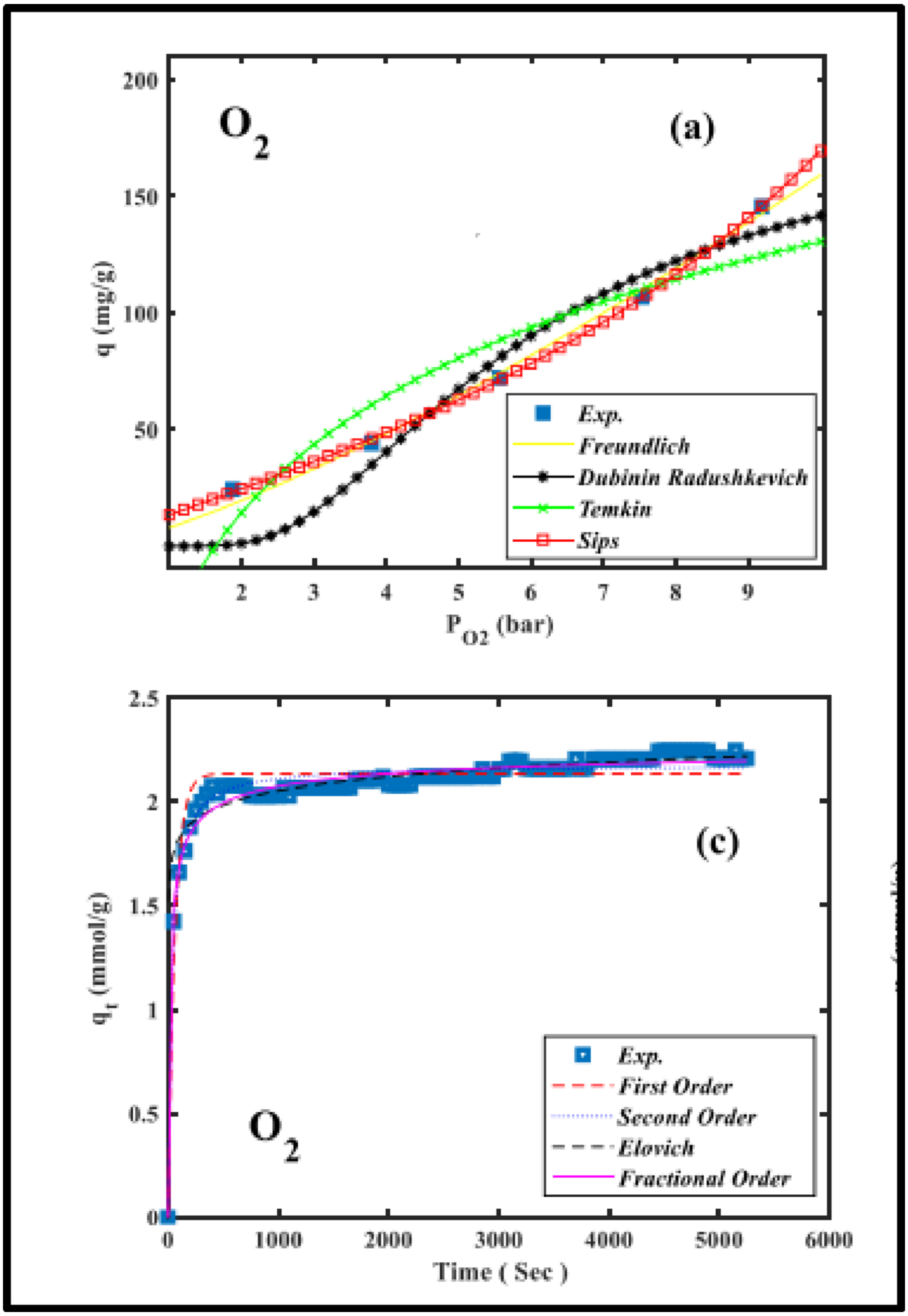

Fig. 6 Oxygen gas adsorption on the W-1000-O sample using fitted isotherm (**a**, **b**) and kinetic (**c**, **d**) models at 298 K (kinetic models under pressure of 6 bar) [153]

selective HMs adsorption, which is usually interfaced with the oxygen functional groups [156].

In order to remove Cu(II), Cr(III), and Pb(II) at the ideal pH (5.0), Niu et al. created a novel fibrous adsorbent chitosan functionalised tetraethylenepentamine (CTPC) using cotton fibres as supporting material. This was done in accordance with the pseudo second-order model kinetics and the Langmuir isotherm, as seen in Fig. 7. Within the first 60 min, the adsorption capacity rose quickly, reaching equilibrium after about 120 min. The pseudo-second-order model was fitted by kinetic data, suggesting that

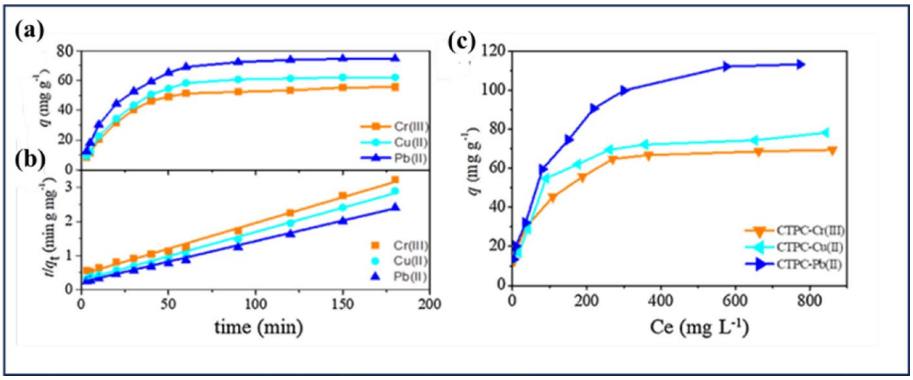

Fig. 7 **a** The effect of contact time on the adsorption capacity of metal ions on the CTPC, **b** the plots of t/qt vs. t for Cu(II), Pb(II) and Cr(III) ions. (initial concentration 300 mg L^{-1}, pH 5.0, 30 °C).**c** Adsorption isotherms of CTPC for Cu(II), Pb(II) and Cr(III) ions (pH 5.0,30 °C) [174].

chemisorption was the predominant mechanism. Monolayer adsorption was demonstrated by Langmuir isotherms, and CTPC showed the highest adsorption capacity for Pb(II) (~115 mg/g), followed by Cu(II) and Cr(III). This demonstrated CTPC's high affinity and selectivity for heavy metals under the conditions under study [174].

Kong et al. fabricated decorated GO with an amino-terminated hyperbranched polymer (HBP-NH_2) using monomers diethylenetriamine (DETA), tetraethylenepentamine (TEPA), triethylenetetramine (TETA) to obtain GO-HBP-NH_2-DETA, GO-HBP-NH_2-TEPA, and GOHBP-NH_2-TETA adsorbents .The Langmuir isotherm model showed high adsorption capabilities of all the three adsorbents towards Cr(VI) [175]. In another study, AC derived from biomass using diammonium hydrogen phosphate (DAP) resulted in dense N-bearing functional groups with a high ratio of micropore structure (>70%). The synthesized AC showed impressive Cr(VI) exclusion from aqueous solutions. The adsorption kinetics and isotherm have been well explained on the basis of the Freundlich model and pseudo second-order kinetics, respectively [176].

Yin et al. studied amino-functionalized MOFs were combined with ceramic membrane ultrafiltration (CUF) for the first time in adsorptive removal of Pb (II) from wastewater. The adsorption capacity at equilibrium was remarkably high (1795.3 mg/g).The pseudo-second-order kinetic model provided the best fit to the adsorption data (R^2 = 0.9997). The adsorption mechanisms of coordination interaction between amidogen (–NH_2) and Pb (II) were confirmed. The adsorbed Pb (II) can be effectively desorbed by controlling pH at 4.5 during 6 cycles [177].The nitrogen-functionalized materials exhibit remarkable affinity for the elimination of an extensive range of HMs viz. Co(II), Cd(II), Cu(II), Ni(II), Pb(II), Cr(VI), and Zn(II) from contaminated water, indicating the strong metal complexing capability of nitrogen groups [178].

4.2.3 Sulfur-based functional groups: thiol and sulfonate

Sulfur-based thiol groups also exhibit affinity towards HMs, similar to oxygen and nitrogen-containing functional groups. A good quantity of studies was conducted on the removal of HMs employing various thiol group-containing adsorbents [179–182]. Depending upon the reaction conditions for surface modification of carbon adsorbents, the rate of inclusion of sulfur-containing functional groups, pore-volume, and surface area can be altered to afford the desired adsorption characteristics. Moreover, loading of elemental sulfur to carbon adsorbents via chemical reaction-deposition and solution infiltration remarkably enhances their adsorption affinity towards different HMs.

Liang et al. observed improved sorption potential of sepiolite for Cd(II) and Pb(II) its functionalization with nano texturization and surface attaching in toluene with mercapto propyl trimethoxy silane [183]. The studies pertaining to the adsorptive removal of HMs by carbon materials bearing sulfur functional groups in terms of their relative capacity of adsorption and isotherm models and the best-fit kinetics are summarized in Table 4.

Pirveysian and Ghiaci synthesized thiol functionalized GO for Pb^{2+}, $Ni^{2+,}$ Cd^{2+} and Zn^{2+} ions removal from water as shown in Fig. 8. Thiol functionalization resulted in enhanced adsorption efficiency owing to the high metal bonding capacity of the thiol groups that are densely immobilized on the surface of functionalized GO. This adsorption phenomenon followed pseudo kinetics, and Langmuir and Redlich Peterson isotherms were best fitted in the study [204].

Feng et al. studied that uninterrupted hydrogen sulfide exposure leads to effective mercury uptake by sorbents owing to the presence of fundamental sulfur types on surfaces of carbonaceous when compared to sulfate and thiophene groups bearing adsorbents. The sulfur-based mesoporous carbons synthesis resulted in adsorbent with improved pore volume (0.71–2.3 cm^3/g) and specific surface area (837–2865 m^2/g), which in turn favors increased adsorption of Hg(II) > Pb(II) > Cd(II) > Ni(II) at pH of 7 [205].

Xia et al. prepared thiol functionalized -aluminum oxide hydroxide (-AlOOH) filters for removal of Pb, Hg, and Cd under non-collateral conditions. For thiol functionalized –AlOOH followed pseudo kinetics and the Lagergren first order; while the behavior of isothermal adsorption for these membranes was best fitted to the both, i.e., Freundlich

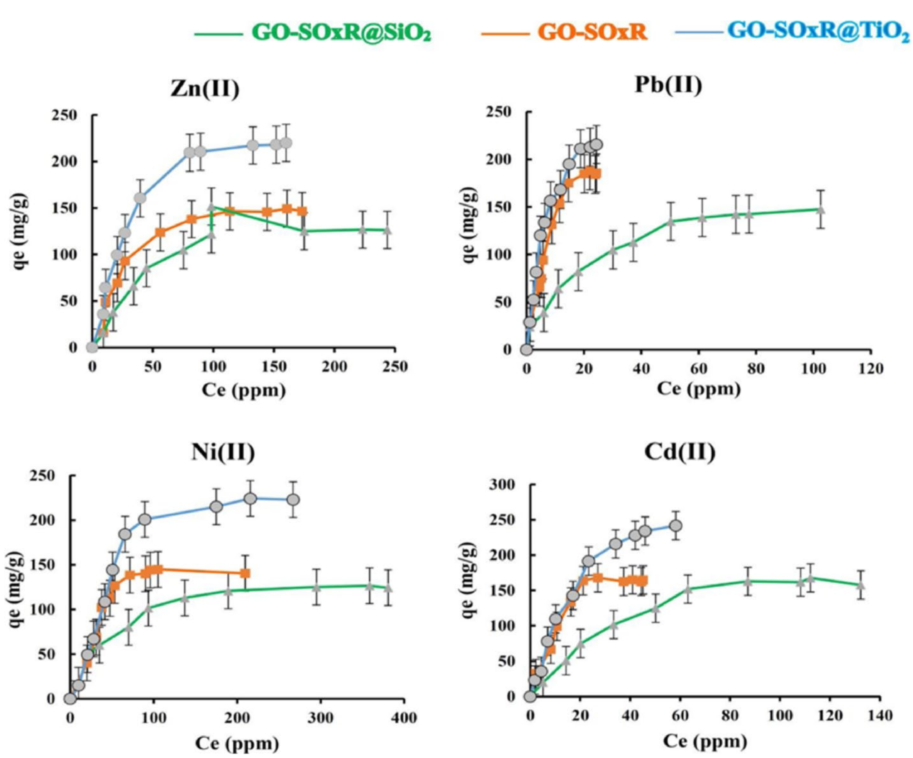

Fig. 8 Equilibrium adsorption of Pb(II), Cd(II), Ni(II), and Zn(II) adsorption on GO-SOxR, GO-SOxR@TiO_2, and GO-SOxR@SiO_2 at 25 °C [204]

Table 5 Carbon-based adsorbents for the removal of HMs with other functional groups

Absorbent	HM (ions)	Functional groups	Adsorption capacity (mg/g)	Isotherm	Kinetic model	References
Iron/carbon (Fe/C) composite prepared by cultivating harmful algal blooms biomass	Cr(VI)	C–H	43	Langmuir	Pseudo-second-order	[211]
Manilkara Zapota tree wood-based AC	Pb(II)	C–H	22	Langmuir	Pseudo-second-order	[212]
Modified-cellulose	Cd(II)	C–C C–H	401.1	Freundlich	Pseudo-second-order	[213]
Hazelnut husk AC prepared with potassium acetate	Cu(II)	C=C C–H	105.3	Langmuir	Pseudo-second-order	[214]
Posidonia oceanica waste	Pb(II)	C–O–C C=C	631.13	Freundlich	Pseudo-second-order	[215]
GO	Cu(II)	C=C	117.5	Freundlich	–	[216]
Ulva lactuca AC	Pb(II)	C=C	83.3	–	–	[217]
Three-dimensional magnetic GO foam/Fe_3O_4 nanocomposite	Cr(IV)	C=C C–C	258.6	Freundlich	–	[218]

model and Langmuir model [206]. Furthermore, Choi et al. suggested that the thiol-functionalized cellulose nanofiber membrane exhibited impressive HMs adsorption. Furthermore, Langmuir isotherm described the capacity of adsorption as a function of adsorbate content which indicated the formation of the surface monolayer by the metal ions with homogenous dispersion of adsorption energy [207].

Pan et al. developed two kinds of sulfhydryl functionalized covalent organic frameworks were obtained via a thiol-ene click reaction between the thiol groups of trithiocyanuric acid (TTC) or bismuththiol (BMT) and vinyl groups on the surface of covalent organic frameworks. Due to their rich sulfur content, both adsorbents (COF-SH-1 and COF-SH-2) exhibited a high level of selective Hg^{2+} removal from aqueous solution with maximum adsorption capacities of 763.4 mg/g and 526.3 mg/g respectively [208].

4.2.4 Emerging functional modifications and their impact

Though HMs removal has been extensively researched using functional groups containing oxygen, sulfur, and nitrogen. Furthermore, the introduction of functional groups such as C=C, $-CH-CH_2$, $-O-CH_3$ to carbon surface has also been found to boost adsorption of HM ions removal. Zubrik et al. prepared coal-based magnetic carbon composites for the exclusion of Cd(II) and As(V) from contaminated water [209]. Kumar et al. developed a fascinating alternative BC-based adsorbent for the uranium U(VI) adsorption from polluted water. The adsorption mechanism strongly suggested pH-dependent aqueous speciation of U(VI) and its adsorption on BC, which was confirmed by the peaks that were noticed at 1424 and 1510 cm^{-1} for lignin in the FTIR [210]. Table 5 summarizes the influence of dissimilar functional groups on carbon for the alteration in the ability of HM ions removal along with the isotherm models and best-fit kinetic and their corresponding adsorption capacity.

5 Challenges and future research directions

Functionalized carbon nanomaterials adsorbents display great promise for HMs removal, but numerous hurdles must be overcome before they can be deployed at real-world and industrial scales. Foremost among these challenges is regeneration and reusability, as many adsorbents degrade structurally after repeated cycles, especially under extreme pH conditions. This highlights the need for chemically robust materials and low-cost, environmentally friendly regeneration strategies that minimize secondary pollution and resource use. Economic and environmental concerns also limit scalability. High synthesis costs, reliance on toxic chemicals, and the lack of large-scale synthesis protocols are key bottlenecks. Additionally, the environmental burden of disposed adsorbents, especially those with bound toxic metals, calls for more research into biodegradable carriers, metal recovery techniques, and safe disposal protocols.While functionalized carbon nanomaterials demonstrate excellent adsorption capacity under controlled laboratory conditions, performance under realistic wastewater environments remains uncertain. These environments contain competing cations (e.g., Ca^{2+}, Mg^{2+}), variable pH, organic matter, and fluctuating contaminant loads, all of which can suppress adsorption efficiency. Moreover, the fate of nanomaterials in aquatic ecosystems is poorly understood; potential leaching and bioaccumulation present risks that require thorough ecotoxicological evaluation.

To guide practical implementation and policy translation, a structured six-phase roadmap is proposed. First, bench-scale screening should assess adsorbent performance in realistic wastewater environments that include multiple competing ions (e.g., Ca^{2+}, Mg^{2+}), variable pH, and natural organic matter. These conditions better represent actual field challenges compared to the idealized lab settings often reported. Both batch and small-scale fixed-bed column experiments should be used to evaluate adsorption kinetics, selectivity, and recyclability under complex matrices. Second, mechanistic validation must employ advanced spectroscopic and microscopic techniques—such as XPS, FTIR, and EXAFS—to elucidate metal binding mechanisms, detect surface fouling, and confirm the stability of functional groups after regeneration. These insights are critical for optimizing surface chemistry and predicting long-term performance. Third, promising materials should undergo pilot-scale testing in continuous-flow systems, such as packed-bed reactors, to assess breakthrough behavior, regeneration feasibility, and operational resilience under dynamic hydraulic conditions. Fourth, life cycle assessment (LCA) and techno-economic analysis (TEA) must be integrated to evaluate energy consumption, synthesis cost, environmental footprint, and metal recovery efficiency. These analyses will identify the most sustainable and cost-effective material designs and processing methods. Fifth, regulatory and safety considerations require in-depth studies on the ecotoxicity, leaching potential, and post-use handling of nanomaterial-laden adsorbents to ensure environmental compliance. Finally, large-scale production and commercialization should involve collaborations with industry partners to develop scalable synthesis protocols, ensure product quality control, and deploy modular systems tailored for decentralized or municipal water treatment applications. This roadmap ensures a comprehensive and interdisciplinary path forward, bridging laboratory success with real-world impact.

6 Conclusion

Functionalized nanocarbon materials have emerged as highly versatile and effective adsorbents for the removal of toxic HMs from aqueous systems. This review systematically evaluated different carbon-based adsorbents—such as GO, CNTs, AC, BC, and emerging 2D materials like g-C_3N_4—with particular focus on surface modifications involving oxygen, nitrogen, and sulfur-containing groups. Among the surveyed materials, oxygen-functionalized graphene and sulfur-doped AC exhibit consistently high adsorption capacities across various metals due to enhanced surface polarity and complexation ability. Nitrogen doping, especially in CNTs and g-C_3N_4 composites, has proven crucial in improving electron donor characteristics, promoting selective binding of cationic species such as Pb(II) and Cr(VI).BC, though less engineered than other nanocarbons, presents a low-cost and tunable platform when functionalized appropriately. Despite these promising advancements, several challenges persist. These include limited adsorption selectivity under competing ions, insufficient studies on adsorbent regeneration and reuse, potential toxicity of carbon nanomaterials in the environment, and the lack of scalable, cost-effective synthesis routes. Moreover, most laboratory investigations are still constrained to batch-scale experiments, which do not fully reflect real-world wastewater complexity. Moving forward, future research must prioritize the design of multifunctional adsorbents capable of selective removal of multiple pollutants, enhance stability and recyclability through surface anchoring or cross-linking strategies, develop green, low-energy synthesis pathways using biomass precursors or waste valorization, and bridge the gap between laboratory studies and field-scale implementations through pilot-scale demonstrations. In conclusion, the integration of material innovation with system-level engineering is essential to realize the full potential of functionalized nanocarbons in environmental remediation. A collaborative approach involving chemists, material scientists, and environmental engineers will be critical to translate laboratory discoveries into practical and sustainable solutions for HMs pollution control.

Acknowledgements
The authors are thankful to IFTM University, Moradabad for their support.

Author contributions
S.T. write the pre-draft of the manuscript. J.K., S.T., and D.K.K. provided the comments, and supervision.

Funding
Not applicable.

Data availability
No datasets were generated or analysed during the current study.

Declarations

Ethics approval and consent to participate
Not applicable.

Consent for publication
Not applicable.

Competing interests
The authors declare no competing interests.

Received: 26 April 2025 / Accepted: 11 February 2026
Published online: 03 March 2026

References

1. Saravanan A, Kumar PS, Jeevanantham S, Anubha M, Jayashree S. Degradation of toxic agrochemicals and pharmaceutical pollutants: effective and alternative approaches toward photocatalysis. Environ Pollut. 2022;298:118844.
2. Joseph L, Jun BM, Flora JR, Park CM, Yoon Y. Removal of heavy metals from water sources in the developing world using low-cost materials: a review. Chemosphere. 2019;229:142–59.
3. Wang D, Wang P, Wang C, Ao Y. Effects of interactions between humic acid and heavy metal ions on the aggregation of TiO_2 nanoparticles in water environment. Environ Pollut. 2019;248:834–44.
4. Yao W, Wang J, Wang P, Wang X, Yu S, Zou Y, Wang X. Synergistic coagulation of GO and secondary adsorption of heavy metal ions on Ca/Al layered double hydroxides. Environ Pollut. 2017;229:827–36.
5. Karthik KV, Raghu AV, Reddy KR, Ravishankar R, Sangeeta M, Shetti NP, Reddy CV. Green synthesis of Cu-doped ZnO nanoparticles and its application for the photocatalytic degradation of hazardous organic pollutants. Chemosphere. 2022;287:132081.
6. Zheng X, Alam O, Zhou Y, Du D, Li G, Zhu W. Heavy metals detection and removal from contaminated water: a critical review of adsorption methods. J Environ Chem Eng. 2024;12:114366.
7. Yang X, Wan Y, Zheng Y, He F, Yu Z, Huang J, Gao B. Surface functional groups of carbon-based adsorbents and their roles in the removal of heavy metals from aqueous solutions: a critical review. Chem Eng J. 2019;366:608–21.
8. Sabzehmeidani MM, Mahnaee S, Ghaedi M, Heidari H, Roy VA. Carbon based materials: a review of adsorbents for inorganic and organic compounds. Mater Adv. 2021;2:598–627.
9. Kumar R, Barakat MA, Taleb MA, Seliem MK. A recyclable multifunctional graphene oxide/SiO_2@ polyaniline microspheres composite for Cu (II) and cr (VI) decontamination from wastewater. J Clean Prod. 2020;268:122290.
10. Tanna AR, Shaik DP, Ramakrishna A. A study on Preparation of nano activated carbon and economical elimination of congo red dyes from aqueous solutions. E3S Web Conf. 2025;619:04007.
11. Abbas Z, Shahid I, Ali S, Naseer MN, Khalid MA, Tabraiz S, Zeeshan M. Graphene and graphene oxide-based nanomaterials as a promising tool for the mitigation of heavy metals from water and wastewater. Membr Technol Heavy Metal Remov Water CRC; 2023;197–222.
12. Anh NN, Minh PN, Van Trinh P, Van Hao N. Graphene oxide–carbon nanotube-magnetite nanocomposites for efficient arsenic removal from aqueous solutions. RSC Adv. 2025;15:20792–809.
13. Ramesha GK, Kumara AV, Muralidhara HB, Sampath S. Graphene and graphene oxide as effective adsorbents toward anionic and cationic dyes. J Colloid Interface Sci. 2011;361:270–7.
14. Taleb MA, Kumar R, Barakat MA. Environmental friendly fabrication of graphene oxide immobilized in chitosan coupled with carboxymethyl cellulose for removal of zinc (II) ions and Oxytetracycline from aqueous solution. Earth Syst Environ. 2025;9:389–402.
15. Neelam. Nanoadsorbents; advanced tailored strategies for precious metals recovery from waste sources. J Mater Sci. 2025;1–22.
16. Zubair M, Roopesh MS, Ullah A. Challenges and prospects: graphene oxide-based materials for water remediation including metal ions and organic pollutants. Environ Sci Nano. 2024;11:3693–720.
17. Zhao G, Li J, Ren X, Chen C, Wang X. Few-layered graphene oxide nanosheets as superior sorbents for heavy metal ion pollution management. Environ Sci Technol. 2011;45:10454–62.
18. Kadari M, Makhlouf M, Khaoua OO, Kesraoui M, Bouriche S, Benmaamar Z. The removal efficiency of cadmium (Cd^{2+}) and lead (Pb^{2+}) from aqueous solution by graphene oxide (GO) and magnetic graphene oxide (α-Fe_2O_3/GO). Chem Afr. 2023;6:1515–28.
19. Promkatkaew M, Srisuratsiri P, Sangpanich U, Somboonviwat K, Kitjaruwankul S. Graphene Oxide–Chitosan composite for efficient adsorptive removal of Cu(II), Co(II), and Ni(II) from simulated E-Waste effluents. ACS Omega. 2025;10:44111–24.
20. Li D, Zhang P, Yang Y, Huang Y, Li T, Yang J. U(VI) adsorption by sodium alginate/graphene oxide composite beads in water. J Radioanal Nucl Chem. 2021;327:1131–41.
21. Sun Y, Wang Q, Chen C, Tan X, Wang X. Interaction between Eu (III) and graphene oxide nanosheets investigated by batch and extended X-ray absorption fine structure spectroscopy and by modeling techniques. Environ Sci Technol. 2012;46:6020–7.
22. Yang X, Hu L, Bai J, Mao X, Chen X, Wang X, Wang S. Increased structural defects of graphene oxide compromised reductive capacity of ZVI towards hexavalent chromium. Chemosphere. 2021;277:130308.
23. Das R, Vecitis CD, Schulze A, Cao B, Ismail AF, Lu X, Chen J, Ramakrishna S. Recent advances in nanomaterials for water protection and monitoring. Chem Soc Rev. 2017;46:6946–7020.
24. Verma B, Balomajumder C. Surface modification of one-dimensional carbon nanotubes: a review for the management of heavy metals in wastewater. Environ Technol Innov. 2020;17:100596.
25. Lan Y, Xu S, Fu Y, Jin L, Han Y, He X, Cui H. The selective adsorption mechanism of heteroatom-doped carbon nanotubes for heavy metals in wastewater. A DFT study. Diam Relat Mater. 2025;152:111875.
26. Yang C, Xue Z, Wen J. Recent advances in MOF-based materials for remediation of heavy metals and organic pollutants: insights into performance, mechanisms, and future opportunities. Sustainability. 2023;15:6686.
27. Esrafili L, Firuzabadi FD, Morsali A, Hu ML. Reuse of predesigned dual-functional metal organic frameworks (DF-MOFs) after heavy metal removal. J Hazard Mater. 2021;403:123696.
28. Burachevskaya M, Minkina T, Bauer T, Lobzenko I, Fedorenko A, Mazarji M, Rajput VD. Fabrication of biochar derived from different types of feedstocks as an efficient adsorbent for soil heavy metal removal. Sci Rep. 2023;13:2020.
29. Zhou Y, Liu W, Chen D, Liu B, Lu P, Zhang Y. Simultaneous remediation of as (V), cd (II) and Pb (II) in aqueous solution and soil using Fe/Ca-modified biochar. Waste Manag Res. 2025;43:1206–18.
30. Liu D, Hao Z, Chen D, Jiang L, Li T, Tian B, Ai H. Use of eggshell-catalyzed biochar adsorbents for Pb removal from aqueous solution. ACS Omega. 2022;7:21808–19.
31. He Y, Jia X, Zhou S, Chen J, Zhang S, Li X, Hu G. Separatable MoS_2 loaded biochar/$CaCO_3$/Alginate gel beads for selective and efficient removal of Pb (II) from aqueous solution. Sep Purif Technol. 2022;303:22212.
32. Wang C, Qiao J, Yuan J, Tang Z, Chu T, Lin R, Tan Y. Novel chitosan-modified biochar prepared from a Chinese herb residue for multiple heavy metals removal: characterization, performance and mechanism. Bioresour Technol. 2024;402:130830.
33. Xie R, Jin Y, Chen Y, Jiang W. The importance of surface functional groups in the adsorption of copper onto walnut shell derived activated carbon. Water Sci Technol. 2017;76:3022–34.

34. Zhu J, Deng B, Yang J, Gang D. Modifying activated carbon with hybrid ligands for enhancing aqueous mercury removal. Carbon. 2009;47:2014–25.
35. Liu WJ, Zeng FX, Jiang H, Zhang XS. Adsorption of lead (Pb) from aqueous solution with typha angustifolia biomass modified by $SOCl_2$ activated EDTA. Chem Eng J. 2011;170:21–8.
36. Yantasee W, Lin Y, Fryxell GE, Alford KL, Busche BJ, Johnson CD. Selective removal of copper (II) from aqueous solutions using fine-grained activated carbon functionalized with amine. Ind Eng Chem Res. 2004;43:2759–64.
37. Xie N, Wang H. Role of oxygen functional groups in Pb^{2+} adsorption from aqueous solution on carbonaceous surface: a density functional theory study. J Hazard Mater. 2021;405:124221.
38. Ali AA, Abdul-Hameed HM. Synthesis and characterization of magnetic activated carbon manufactured from palm stones by physical activation to remove lead from aqueous solution. Desalin Water Treat. 2025;321:100951.
39. Yuan X, An N, Zhu Z, Sun H, Zheng J, Jia M, Liu N. Hierarchically porous nitrogen-doped carbon materials as efficient adsorbents for removal of heavy metal ions. Process Saf Environ Prot. 2018;119:320–9.
40. Yang J, Song H, Zhang Y, Zhu X. Preparation of functionalization graphite carbonitride photocatalytic membrane and its application in degradation of organic pollutants. Surf Interfaces. 2021;24:101092.
41. Taleb MA, Kumar R, Abdelbaky NF, Barakat MA. Nanostructured aerogels for adsorptive removal of pharmaceutical pollutants from wastewater: a review on synthesis and application. J Environ Chem Eng. 2024;12:114538.
42. Wang B, Gao B, Fang J. Recent advances in engineered biochar productions and applications. Crit Rev Environ Sci Technol. 2017;47:2158–207.
43. Lyu H, Gao B, He F, Ding C, Tang J, Crittenden JC. Ball-milled carbon nanomaterials for energy and environmental applications. ACS Sustain Chem Eng. 2017;5:9568–85.
44. Machida M, Fotoohi B, Amamo Y, Ohba T, Kanoh H, Mercier L. Cadmium (II) adsorption using functional mesoporous silica and activated carbon. J Hazard Mater. 2012;221:220–7.
45. Kumar R, Ansari MO, Taleb MA, Oves M, Barakat MA, Alghamdi MA, Al Makishah NH. Integrated adsorption-photocatalytic decontamination of oxytetracycline from wastewater using S-doped TiO_2/WS_2/calcium alginate beads. Catalysts. 2022;12:1676.
46. Hadi P, To MH, Hui CW, Lin CSK, McKay G. Aqueous mercury adsorption by activated carbons. Water Res. 2015;73:37–55.
47. Taleb MA, Kumar R, Barakat MA. Multifunctional carboxymethyl cellulose/graphene oxide/polyaniline hybrid thin film for adsorptive removal of Cu (II) and oxytetracycline antibiotic from wastewater. Int J Biol Macromol. 2023;253:126699.
48. Huang D, Wu J, Wang L, Liu X, Meng J, Tang X, Xu J. Novel insight into adsorption and co-adsorption of heavy metal ions and an organic pollutant by magnetic graphene nanomaterials in water. Chem Eng J. 2019;358:1399–409.
49. Cao F, Lian C, Yu J, Yang H, Lin S. Study on the adsorption performance and competitive mechanism for heavy metal contaminants removal using novel multi-pore activated carbons derived from recyclable long-root *Eichhornia crassipes*. Bioresour Technol. 2019;276:211–8.
50. Borras A, Henriques B, Goncalves G, Fraile J, Pereira E, Lopez-Periago AM, Domingo C. Graphene oxide/polyethylenimine aerogels for the removal of hg (II) from water. Gels. 2022;8:452.
51. Shariful MI, Sepehr T, Mehrali M, Ang BC, Amalina MA. Adsorption capability of heavy metals by chitosan/poly (ethylene oxide)/activated carbon electrospun nanofibrous membrane. J Appl Polym Sci. 2018;135:45851.
52. Zhang Y, Chi H, Zhang W, Sun Y, Liang Q, Gu Y, Jing R. Highly efficient adsorption of copper ions by a PVP-reduced graphene oxide based on a new adsorptions mechanism. Nano-Micro Lett. 2014;6:80–7.
53. Mishra S, Dwivedi J, Kumar A, Sankararamakrishnan N. Removal of antimonite (Sb (III)) and antimonate (Sb (V)) using zerovalent iron decorated functionalized carbon nanotubes. RSC Adv. 2016;6:95865–78.
54. Thuan LV, Chau TB, Ngan TTK, Vu TX, Nguyen DD, Nguyen MH, Sinh LH. Preparation of cross-linked magnetic chitosan particles from steel slag and shrimp shells for removal of heavy metals. Environ Technol. 2018;39:1745–52.
55. Kyzas GZ, Bomis G, Kosheleva RI, Efthimiadou EK, Favvas EP, Kostoglou M, Mitropoulos AC. Nanobubbles effect on heavy metal ions adsorption by activated carbon. Chem Eng J. 2019;356:91–7.
56. Mudassar H, Hina K, Ghani U, Afzaal Q, Shah AA, Shaffique S, Elansary HO. Adsorptive removal of Pb^{2+} from wastewater using ZnO-Biochar nanocomposite. Sci Rep. 2025;15:29517.
57. Li Y, Xia M, An F, Ma N, Jiang X, Zhu S, Ma J. Superior removal of hg (II) ions from wastewater using hierarchically porous, functionalized carbon. J Hazard Mater. 2019;371:33–41.
58. Li Y, Zhao B, Shang T. Adsorption of copper(II) in biochar–humic acid–water system. Sci Rep. 2025;15:24948.
59. Alizadeh B, Ghorbani M, Salehi MA. Application of polyrhodanine modified multi-walled carbon nanotubes for high efficiency removal of Pb (II) from aqueous solution. J Mol Liq. 2016;220:142–9.
60. Huang L, He M, Chen B, Hu B. Magnetic Zr-MOFs nanocomposites for rapid removal of heavy metal ions and dyes from water. Chemosphere. 2018;199:435–44.
61. Jiang SY, He WW, Li SL, Su ZM, Lan YQ. Introduction of molecular building blocks to improve the stability of metal–organic frameworks for efficient mercury removal. Inorg Chem. 2018;57:6118–23.
62. Heryanto H, Tahir D, Abdullah B, Kavgaci M, Rinovian A, Masrour R, Sayyed MI. Carbon as a multifunctional material in supporting adsorption performance for water treatment: science mapping and review. Desalin Water Treat. 2024;320:100758.
63. Rajendran S, Priya AK, Kumar PS, Hoang TK, Sekar K, Chong KY, Show PL. A critical and recent developments on adsorption technique for removal of heavy metals from wastewater-A review. Chemosphere. 2022;303:135146.
64. Aziz KHH. Removal of toxic heavy metals from aquatic systems using low-cost and sustainable biochar: a review. Desalin Water Treat. 2024;320:100757.
65. Gęca M, Khalil AM, Tang M, Bhakta AK, Snoussi Y, Nowicki P, Chehimi MM. Surface treatment of biochar—methods, surface analysis and potential applications: a comprehensive review. Surfaces. 2023;6:179–213.
66. Zhao W, Adeel M, Zhang P, Zhou P, Huang L, Zhao Y, Rui Y. A critical review on surface-modified nano-catalyst application for the photocatalytic degradation of volatile organic compounds. Environ Sci Nano. 2022;9:061–80.
67. Qasem NA, Mohammed RH, Lawal DU. Removal of heavy metal ions from wastewater: a comprehensive and critical review. Npj Clean Water. 2021;4:36.
68. Abd Elnabi MK, Elkaliny NE, Elyazied MM, Azab SH, Elkhalifa SA, Elmasry S, Mahmoud YAG. Toxicity of heavy metals and recent advances in their removal: a review. Toxics. 2023;11:580.

69. Melliti A, Yılmaz M, Sillanpaa M, Hamrouni B, Vurm R. Low-cost date palm fiber activated carbon for effective and fast heavy metal adsorption from water: characterization, equilibrium, and kinetics studies. Colloids Surf A: Physicochem. 2023;672:131775.
70. Ugwu EI, Othmani A, Nnaji CC. A review on zeolites as cost-effective adsorbents for removal of heavy metals from aqueous environment. Int J Environ Sci Technol. 2022;19:8061–84.
71. Basu A, Ali SS, Hossain SS, Asif M. A review of the dynamic mathematical modeling of heavy metal removal with the biosorption process. Processes. 2022;10:1154.
72. Raji Z, Karim A, Karam A, Khalloufi S. Adsorption of heavy metals: mechanisms, kinetics, and applications of various adsorbents in wastewater remediation—a review. Waste. 2023; l:775-05.
73. Adamczyk Z, Warszynski P. Role of electrostatic interactions in particle adsorption. Adv Colloid Interface Sci. 1996;63:41–149.
74. Hu Y, Guo T, Ye X, Li Q, Guo M, Liu H, Wu Z. Dye adsorption by resins: effect of ionic strength on hydrophobic and electrostatic interactions. Chem Eng J. 2013;228:392–7.
75. Aljamali NM, Khdur R, Alfatlawi IO. Physical and chemical adsorption and its applications. Int J Thermodyn Chem Kinet. 2021;7:1–8.
76. Alaqarbeh M. Adsorption phenomena: definition, mechanisms, and adsorption types: short review. RHAZES Green Appl Chem. 2021;13:43–51.
77. Held PA, Fuchs H, Studer A. Covalent-Bond formation via On-Surface chemistry. Chem Eur J. 2017;23:5874–92.
78. Liu T, Han X, Wang Y, Yan L, Du B, Wei Q, Wei D. Magnetic chitosan/anaerobic granular sludge composite: synthesis, characterization and application in heavy metal ions removal. J Colloid Interface Sci. 2017;508:405–14.
79. Li Y, Liu F, Xia B, Du Q, Zhang P, Wang D, Xia Y. Removal of copper from aqueous solution by carbon nanotube/calcium alginate composites. J Hazard Mater. 2010;177:876–80.
80. Li H, Xiong J, Zhang G, Liang A, Long J, Xiao T, Zhang H. Enhanced thallium (I) removal from wastewater using hypochlorite oxidation coupled with magnetite-based biochar adsorption. Sci Total Environ. 2020;698:134166.
81. Ismail UM, Vohra MS, Onaizi SA. Adsorptive removal of heavy metals from aqueous solutions: progress of adsorbents development and their effectiveness. Environ Res. 2024;251:118562.
82. Wang H, Gao B, Fang J, Ok YS, Xue Y, Yang K, Cao, X. Engineered biochar derived from eggshell-treated biomass for removal of aqueous lead. Ecol Eng. 2018;121:124–9.
83. Zhang X, Yan L, Li J, Yu H. Adsorption of heavy metals by l-cysteine intercalated layered double hydroxide: kinetic, isothermal and mechanistic studies. J Colloid Interface Sci. 2020;562:149–58.
84. Miyah Y, El Messaoudi N, Benjelloun M, Acikbas Y, Şenol ZM, Ciğeroğlu Z, Lopez-Maldonado EA. Advanced applications of hydroxyapatite nanocomposite materials for heavy metals and organic pollutants removal by adsorption and photocatalytic degradation: a review. Chemosphere. 2024;358:142236.
85. Hayat A, Rauf S, Al Alwan B, El Jery A, Almuqati N, Melhi S, Lv W. Recent advance in MOFs and MOF-based composites: synthesis, properties, and applications. Mater Today Energy. 2024;41:101542.
86. He M, Zhang Z, Wang M, Liang C, Wang H, Cheng C, Zhang Z. A review of hydroxyapatite synthesis for heavy metal adsorption assisted by machine learning. J Hazard Mater. 2025;481:136525.
87. Bandara PC, Peña-Bahamonde J, Rodrigues DF. Redox mechanisms of conversion of cr (VI) to cr (III) by graphene oxide-polymer composite. Sci Rep. 2020;10:9237.
88. ALSamman MT, Sotelo S, Sanchez J, Rivas BL. Arsenic oxidation and its subsequent removal from water: an overview. Sep Purif Technol. 2023;309:123055.
89. Ali I, Peng C, Lin D, Saroj DP, Naz I, Khan ZM, Ali M. Encapsulated green magnetic nanoparticles for the removal of toxic Pb^{2+} and Cd^{2+} from water: development, characterization and application. J Environ Manage. 2019;234:273–89.
90. Nure JF, Nkambule TT. The recent advances in adsorption and membrane separation and their hybrid technologies for micropollutants removal from wastewater. J Ind Eng Chem. 2023;126:92–114.
91. Sajid M, Asif M, Baig N, Kabeer M, Ihsanullah I, Mohammad AW. Carbon nanotubes-based adsorbents: properties, functionalization, interaction mechanisms, and applications in water purification. J Water Process Eng. 2022;47:102815.
92. Dev VV, Nair KK, Baburaj G, Krishnan KA. Pushing the boundaries of heavy metal adsorption: a commentary on strategies to improve adsorption efficiency and modulate process mechanisms. Colloid Interfac Sci. 2022;49:100626.
93. Alahmer A, Ajib S, Wang X. Comprehensive strategies for performance improvement of adsorption air conditioning systems: a review. Renew Sustain Energy Rev. 2019;99:138–58.
94. Joshi M, Bhatt D, Srivastava A. Enhanced adsorption efficiency through Biochar modification: a comprehensive review. Ind Eng Chem Res. 2023;62:13748–61.
95. Abegunde SM, Idowu KS, Adejuwon OM, Adeyemi-Adejolu T. A review on the influence of chemical modification on the performance of adsorbents. Resour Environ Sustain. 2020;1:100001.
96. Du M, Zhang Y, Wang Z, Lv M, Tang A, Yu Y, Li A. Insight into the synthesis and adsorption mechanism of adsorbents for efficient phosphate removal: exploration from synthesis to modification. Chem Eng J. 2022;442:136147.
97. Qiu B, Shao Q, Shi J, Yang C, Chu H. Application of Biochar for the adsorption of organic pollutants from wastewater: modification strategies, mechanisms and challenges. Sep Purif Technol. 2022;300:121925.
98. Schertenleib T, Karve VV, Stoian D, Asgari M, Trukhina O, Oveisi E, Queen WL. A post-synthetic modification strategy for enhancing Pt adsorption efficiency in MOF/polymer composites. Chem Sci. 2024;15:8323–33.
99. Donga C, Mishra SB, Ndlovu LN, Abd-El-Aziz AS, Kuvarega AT, Mishra AK. Magnetic magnetite-graphene oxide (Fe_3O_4-GO) nanocomposites for removal of dyes from aqueous solution. J Inorg Organomet Polym. 2024;34:4192–202.
100. Hamda AS, Areti HA, Gudeta RL, Abo LD, Jayakumar M. Carbon-based nanomaterials for water treatment: a comprehensive review of recent advances and mechanisms. Chem Eng J Adv. 2025;100834.
101. Dinh VC, Hou CH, Dao TN. O, N-doped porous Biochar by air oxidation for enhancing heavy metal removal: the role of O, N functional groups. Chemosphere. 2022;293:133622.
102. Ahuja R, Kalia A, Sikka R, Chaitra P. Nano modifications of Biochar to enhance heavy metal adsorption from wastewaters: a review. ACS Omega. 2022;7:45825–36.
103. Xie Z, Diao S, Xu R, Wei G, Wen J, Hu G, Huang H. Construction of carboxylated-GO and MOFs composites for efficient removal of heavy metal ions. Appl Surf Sci. 2023;636:157827.

104. Li X, Liu Y, Zhang C, Wen T, Zhuang L, Wang X. Porous Fe_2O_3 microcubes derived from metal organic frameworks for efficient elimination of organic pollutants and heavy metal ions. Chem Eng J. 2018;336:241–52.
105. Al-Khaldi FA, Abusharkh B, Khaled M, Atieh MA, Nasser MS, Saleh TA, Gupta VK. Adsorptive removal of cadmium (II) ions from liquid phase using acid modified carbon-based adsorbents. J Mol Liq. 2015;204:255–63.
106. Imran M, Khan ZUH, Iqbal MM, Iqbal J, Shah NS, Munawar S, Rizwan M. Effect of Biochar modified with magnetite nanoparticles and HNO_3 for efficient removal of cr (VI) from contaminated water: a batch and column scale study. Environ Pollut. 2020;261:114231.
107. Lin S, Huang W, Yang H, Sun S, Yu J. Recycling application of waste long-root *Eichhornia crassipes* for heavy metal removal using oxidized Biochar as an adsorbent. Bioresour Technol. 2020;314:123749.
108. Khandaker S, Toyohara Y, Kamida S. Adsorptive removal of cesium from aqueous solution using oxidized bamboo charcoal. Water Resour Ind. 2018;19:35–46.
109. Tu B, Wen R, Wang K, Cheng Y, Deng Y, Cao W, Tao H. Efficient removal of aqueous hexavalent chromium by activated carbon derived from Bermuda grass. J Colloid Interface Sci. 2020;560:649–58.
110. Zhao Z, Xie B, Wang X, Wang Q, Guo C, Zhang F, Zhang C. Adaptive growth strategies of *Quercus dentata* to drought and nitrogen enrichment: a physiological and biochemical perspective. Front Plant Sci. 2024;15:1479563.
111. Kaur M, Kaur M, Singh D, Feng M, Sharma VK. Magnesium ferrite–nitrogen-doped graphene oxide nanocomposite for effective adsorptive removal of lead(II) and arsenic(III). Environ Sci Pollut Res. 2022;29:48260–75.
112. Kurig N, Palkovits R. Electrochemical nitration for organic C–N bond formation: a current view on possible N-sources, mechanisms, and technological feasibility. Green Chem. 2023;25:7508–17.
113. Yu C, Liu M, Song M, Xu X, Zong N, Zhu J, Shi P. Nitrogen enrichment enhances competition for nitrogen uptake between *Stipa purpurea* and microorganisms in a tibetan alpine steppe. Plant Soil. 2023;488:503–16.
114. Wang J, Zheng S, Shao Y, Liu J, Xu Z, Zhu D. Amino-functionalized $Fe_3O_4@SiO_2$ core–shell magnetic nanomaterial as a novel adsorbent for aqueous heavy metal removal. J Colloid Interface Sci. 2010;349:293–9.
115. Pei H, Wang J, Yang Q, Yang W, Hu N, Suo Y, Wang J. Interfacial growth of nitrogen-doped carbon with multifunctional groups on a MoS_2 skeleton for efficient Pb(II) removal. Sci Total Environ. 2018;631:912–20.
116. Shao D, Chen C, Wang X. Application of polyaniline and multiwalled carbon nanotube magnetic composites for removal of Pb(II). Chem Eng J. 2012;185:144–50.
117. Yin N, Wang K, Xia YA. Novel melamine-modified metal–organic frameworks for remarkably high removal of Pb(II). Desalination. 2018;430:120–7.
118. Zhang L, Wang J, Du T, Zhang W, Zhu W, Yang C, Wang J. NH_2-MIL-53(Al) metal–organic framework as a smart platform for simultaneous high-performance detection and removal of Hg^{2+}. Inorg Chem. 2019;58:12573–81.
119. Guo S, Wang Y, Wei X, Gao Y, Xiao B, Yang Y. Structural analysis and heavy metal adsorption of N-doped Biochar from hydrothermal carbonization of *Camellia sinensis* waste. Environ Sci Pollut Res. 2020;27:18866–74.
120. Chu B, Amano Y, Machida M. Preparation of bean dreg-derived N-doped activated carbon with high adsorption capacity for Cr(VI). Colloids Surf Physicochem Eng Asp. 2020;586:124262.
121. Geng J, Yin Y, Liang Q, Zhu Z, Luo H. Polyethyleneimine cross-linked graphene oxide for removing hazardous hexavalent chromium: adsorption performance and mechanism. Chem Eng J. 2019;361:1497–510.
122. Zheng W, Chen S, Liu H, Ma Y, Xu W. Study of the modification mechanism of heavy metal ions adsorbed by biomass-activated carbon doped with a solid nitrogen source. RSC Adv. 2019;9:37440–9.
123. Yin M, Bai X, Wu D, Li F, Jiang K, Ma N, Fang L. Sulfur-functional group tuning on biochar through sodium thiosulfate-modified molten salt processing for efficient heavy metal adsorption. Chem Eng J. 2022;433:134441.
124. Li X, Ma W, Li H, Zhang Q, Liu H. Sulfur-functionalized metal–organic frameworks: synthesis and applications as advanced adsorbents. Coord Chem Rev. 2020;408:213191.
125. Liu Y, Wang Y, Li X, Zhang X, Fang M, Zheng L, Wang T. Multipath accelerated sulfadiazine degradation via peracetic acid oxidation induced by nanoconfined Co species: highlighting the electron rearrangement effect. Chem Eng J. 2024;494:153167.
126. Lu XG, Guo YT. Removal of Pb(II) from aqueous solution by sulfur-functionalized walnut shell. Environ Sci Pollut Res. 2019;26:12776–87.
127. Wu Z, Cheng Z. Adsorption of Pb(II) from glucose solution on thiol-functionalized cellulosic biomass. Bioresour Technol. 2012;104:807–9.
128. Das SK, Shome I, Guha AK. Surface functionalization of *Aspergillus versicolor* mycelia: in situ fabrication of cadmium sulfide nanoparticles and removal of cadmium ions from aqueous solution. RSC Adv. 2012;2:3000–7.
129. Fayazi M. Removal of mercury(II) from wastewater using a sulfur-coated magnetic carbon nanotube composite. Environ Sci Pollut Res. 2020;27:12270–9.
130. Algieri V, Tursi A, Costanzo P, Maiuolo L, De Nino A, Nucera A, Beneduci A. Thiol-functionalized cellulose for mercury polluted water remediation: synthesis and study of the adsorption properties. Chemosphere. 2024;355:141891.
131. Rodríguez C, Leiva E. Enhanced heavy metal removal from acid mine drainage wastewater using double-oxidized multiwalled carbon nanotubes. Molecules. 2019;25:111.
132. Binazir IA, Vafa N, Firoozabadi B. Layered graphene oxide membrane for heavy metal separation via molecular dynamics simulation. J Mol Liq. 2025;417:126639.
133. Bai J, Sun H, Yin X, Yin X, Wang S, Creamer AE, Gao B. Oxygen-content-controllable graphene oxide from electron-beam-irradiated graphite: synthesis, characterization, and removal of aqueous lead [Pb(II)]. ACS Appl Mater Interfaces. 2016;8:25289–96.
134. Chen H, Meng Y, Jia S, Hua W, Cheng Y, Lu J, Wang H. Graphene oxide-modified waste newspaper for removal of heavy metal ions and its application in industrial wastewater. Mater Chem Phys. 2020;244:122692.
135. Ragheb E, Shamsipur M, Jalali F, Mousavi F. Modified magnetic metal–organic framework as a green and efficient adsorbent for removal of heavy metals. J Environ Chem Eng. 2022;10:107297.
136. Joshi AA, Ragupathy G. Performance and mechanisms of waste-based carbon adsorbents in heavy metal removal–an experimental and theoretical approach. RSC Adv. 2025;15:34609–34.
137. Tan M, Liu X, Li W, Li H. Enhancing sorption capacities for copper(II) and lead(II) under weakly acidic conditions using L-tryptophan-functionalized graphene oxide. J Environ Chem Eng. 2015;3:1469–75.

138. Liu J, Liu W, Wang Y, Xu M, Wang B. A novel reusable nanocomposite adsorbent, xanthated Fe_3O_4–chitosan grafted onto graphene oxide, for removing Cu(II) from aqueous solutions. Appl Surf Sci. 2016;367:327–34.
139. Li B, Yang L, Wang CQ, Zhang QP, Liu QC, Li YD, Xiao R. Adsorption of Cd(II) from aqueous solutions by rape straw biochar derived from different modification processes. Chemosphere. 2017;175:332–40.
140. Chen G, Liu Y, Liu F, Zhang X. Fabrication of three-dimensional graphene foam with high electrical conductivity and large adsorption capability. Appl Surf Sci. 2014;311:808–15.
141. Jin J, Li S, Peng X, Liu W, Zhang C, Yang Y, Wang X. HNO_3-modified biochars for uranium(VI) removal from aqueous solution. Bioresour Technol. 2018;256:247–53.
142. Bohli T, Ouederni A. Improvement of oxygen-containing functional groups on olive stone activated carbon by ozone and nitric acid for heavy metal removal from aqueous phase. Environ Sci Pollut Res. 2016;23:15852–61.
143. Jin H, Capareda S, Chang Z, Gao J, Xu Y, Zhang J. Biochar pyrolytically produced from municipal solid waste for aqueous As(V) removal: adsorption properties and improvement by KOH activation. Bioresour Technol. 2014;169:622–9.
144. Zuo X, Liu Z, Chen M. Effect of H_2O_2 concentration on copper removal using modified hydrothermal Biochar. Bioresour Technol. 2016;207:262–7.
145. Tang W, Cai N, Xie H, Liu Y, Wang Z, Liao Y, Yin D. Efficient adsorption removal of Cd(II) from aqueous solutions by HNO_3-modified bamboo-derived Biochar. IOP Conf Ser Mater Sci Eng. 2020;729:012081.
146. Mashhadi S, Sohrabi R, Javadian H, Ghasemi M, Tyagi I, Agarwal S, Gupta VK. Rapid removal of Hg(II) from aqueous solution by rice straw activated carbon prepared by microwave-assisted H_2SO_4 activation: kinetic, isotherm and thermodynamic studies. J Mol Liq. 2016;215:144–53.
147. Chen JH, Xing HT, Guo HX, Weng W, Hu SR, Li SX, Su ZB. Adsorption properties of Cr(VI) ions on a novel graphene oxide-based composite adsorbent. J Mater Chem A. 2014;2:12561–70.
148. Wang N, Zheng P, Ma X. Modification of carbon materials with carbon disulfide for Pb(II) removal. Powder Technol. 2016;301:1–9.
149. Farghali AA, Abdel Tawab HA, Abdel Moaty SA, Khaled R. Functionalization of acidified multiwalled carbon nanotubes for removal of heavy metals from aqueous solutions. J Nanostruct Chem. 2017;7:101–11.
150. Zeng T, Yu Y, Li Z, Zuo J, Kuai Z, Jin Y, Peng C. 3D MnO_2 nanotubes@reduced graphene oxide hydrogel as a reusable adsorbent for heavy metal ion removal. Mater Chem Phys. 2019;231:105–8.
151. Fan Q, Sun J, Chu L, Cui L, Quan G, Yan J, Iqbal M. Effects of chemical oxidation on surface oxygen-containing functional groups and adsorption behavior of Biochar. Chemosphere. 2018;207:33–40.
152. Lu M, Li L, Shen S, Chen D, Han W. Highly efficient Pb(II) removal by a sandwich-structured metal–organic framework/graphene oxide composite with enhanced stability. New J Chem. 2019;43:1032–7.
153. Mashhadimoslem H, Ghaemi A, Maleki A, Elkamel A. Enhancement of oxygen adsorption using biomass-based oxidized porous carbon. J Environ Chem Eng. 2023;11:109300.
154. Wu J, Wang T, Zhang Y, Pan WP. Distribution of Pb(II) and Cd(II) adsorption mechanisms on biochars from aqueous solution considering increased oxygen functional groups induced by HCl treatment. Bioresour Technol. 2019;291:121859.
155. Zhou N, Chen H, Xi J, Yao D, Zhou Z, Tian Y, Lu X. Biochars with excellent Pb(II) adsorption properties produced from fresh and dehydrated banana peels via hydrothermal carbonization. Bioresour Technol. 2017;232:204–10.
156. Cheng S, Zeng X, Liu P. One-step synthesis of magnetic N-doped carbon nanotubes derived from waste plastics for effective Cr(VI) removal. Arab J Chem. 2024;17:105956.
157. Arshad F, Selvaraj M, Zain J, Banat F, Haija MA. Polyethylenimine-modified graphene oxide hydrogel composite as an efficient adsorbent for heavy metal ions. Sep Purif Technol. 2019;209:870–80.
158. Li P, Wang J, Li X, Zhu W, He S, Han C, Dionysiou DD. Facile synthesis of amino-functionalized large-size mesoporous silica spheres and their application for Pb(II) removal. J Hazard Mater. 2019;378:120664.
159. Zhan W, Gao L, Fu X, Siyal SH, Sui G, Yang X. Green synthesis of amino-functionalized carbon nanotube–graphene hybrid aerogels for high-performance heavy metal ion removal. Appl Surf Sci. 2019;467:1122–33.
160. Chen Y, Zhao W, Zhao H, Dang J, Jin R, Chen Q. Efficient removal of Pb(II), Cd(II), Cu(II), and Ni(II) from aqueous solutions by tetrazole-bonded bagasse. Chem Phys. 2020;529:110550.
161. Liu J, Chen TW, Yang YL, Bai ZC, Xia LR, Wang M, Li L. Removal of heavy metal ions and anionic dyes from aqueous solutions using amide-functionalized cellulose-based adsorbents. Carbohydr Polym. 2020;230:115619.
162. Veličković Z, Vuković GD, Marinković AD, Moldovan MS, Perić-Grujić AA, Uskoković PS, Ristić MĐ. Adsorption of arsenate on iron(III) oxide-coated ethylenediamine-functionalized multiwalled carbon nanotubes. Chem Eng J. 2012;181:174–81.
163. Guo Z, Zhang X, Kang Y, Zhang J. Biomass-derived carbon sorbents for Cd(II) removal: activation and adsorption mechanism. ACS Sustain Chem Eng. 2017;5:4103–9.
164. Yang G, Tang L, Zeng G, Cai Y, Tang J, Pang Y, Xiong W. Simultaneous removal of lead and phenol from water by nitrogen-functionalized magnetic ordered mesoporous carbon. Chem Eng J. 2015;259:854–64.
165. Oyetade OA, Skelton AA, Nyamori VO, Jonnalagadda SB, Martincigh BS. Experimental and DFT studies on selective adsorption of Pb(II) and Zn(II) from aqueous solution by nitrogen-functionalized multiwalled carbon nanotubes. Sep Purif Technol. 2017;188:174–87.
166. Oyetade OA, Nyamori VO, Martincigh BS, Jonnalagadda SB. Nitrogen-functionalized carbon nanotubes as a novel adsorbent for Cu(II) removal from aqueous solution. RSC Adv. 2016;6:2731–45.
167. Zhang K, Li H, Xu X, Yu H. Facile and efficient synthesis of nitrogen-functionalized graphene oxide as a copper adsorbent and its application. Ind Eng Chem Res. 2016;55:2328–35.
168. El-Nemr MA, Aigbe UO, Ukhurebor KE, Obodo KO, Awe AA, Hassaan MA, Ragab S, El Nemr A. Modelling of a new form of nitrogen-doped activated carbon for adsorption of various dyes and hexavalent chromium ions. Sci Rep. 2025;15:3896.
169. Mi B, Wang Y. Performance and mechanism of porous carbons derived from biomass as adsorbent for removal of Cr(VI). Processes. 2024;12:2229.
170. Mian MM, Liu G, Yousaf B, Fu B, Ullah H, Ali MU, Ruijia L. Simultaneous functionalization and magnetization of biochar via NH_3-atmosphere pyrolysis for efficient Cr(VI) removal. Chemosphere. 2018;208:712–21.
171. Huang Q, Liu M, Deng F, Wang K, Huang H, Xu D, Wei Y. Mussel-inspired preparation of amine-functionalized Kaolin for effective removal of heavy metal ions. Mater Chem Phys. 2016;181:116–25.
172. Saleem H, Rafique U, Davies RP. Post-synthetically modified UiO-66-NH_2 for adsorptive removal of heavy metal ions from aqueous solution. Microporous Mesoporous Mater. 2016;221:238–44.

173. Yang Z, Dong Y, Meng X, Yang X, Hu R, Liu Y, Wu J. Nitrogen-functionalized bone chars with developed surface area for efficient adsorption of multiple aquatic pollutants. Colloids Surf Physicochem Eng Asp. 2022;647:129061.
174. Niu Y, Hu W, Guo M, Wang Y, Jia J, Hu Z. Preparation of cotton-based fibrous adsorbents for removal of heavy metal ions. Carbohydr Polym. 2019;225:115218.
175. Kong Q, Wei J, Hu Y, Wei C. Fabrication of terminal amino hyperbranched polymer-modified graphene oxide and its prominent adsorption performance toward Cr(VI). J Hazard Mater. 2019;363:161–9.
176. Guo Z, Zhang J, Liu H, Kang Y. Development of a nitrogen-functionalized carbon adsorbent derived from biomass waste by diammonium hydrogen phosphate activation for Cr(VI) removal. Powder Technol. 2017;318:459–64.
177. Yin H, Wang B, Zhang M, Zhang F. Adsorption of Pb(II) from water by modified chitosan-based microspheres and mechanism study. Int J Biol Macromol. 2024;277:134062.
178. Lin S, Liu L, Yang Y, Lin K. Preferential adsorption of cationic heavy metals using amine-functionalized magnetic iron oxide nanoparticles as efficient adsorbents. Appl Surf Sci. 2017;407:29–35.
179. Hezarjaribi M, Bakeri G, Sillanpää M, Chaichi MJ, Akbari S, Rahimpour A. Novel adsorptive PVC nanofibrous/thiol-functionalized TNT composite ultrafiltration membranes for dynamic removal of heavy metal ions. J Environ Manag. 2021;284:111996.
180. Choi HY, Bae JH, Hasegawa Y, An S, Kim IS, Lee H, Kim M. Thiol-functionalized cellulose nanofiber membranes for effective adsorption of heavy metal ions from water. Carbohydr Polym. 2020;234:115881.
181. Lv H, Zhang F, Sun J, Huang S, Wang C. Eco-friendly thiol-functionalized magnetic oxygenous carbon nitride nanocomposites for effective elimination of heavy metals. J Clean Prod. 2024;472:143475.
182. Dobrzynska J. Amine- and thiol-functionalized SBA-15 as potential materials for As(V), Cr(VI), and Se(VI) removal from water: a comparative study. J Water Process Eng. 2021;40:101942.
183. Liang X, Xu Y, Sun G, Wang L, Sun Y, Sun Y, Qin X. Preparation and characterization of mercapto-functionalized sepiolite and its application for sorption of lead and cadmium. Chem Eng J. 2011;174:436–44.
184. Park JH, Wang JJ, Zhou B, Mikhael JE, DeLaune RD. Removal of mercury from aqueous solution using sulfurized biochar and associated mechanisms. Environ Pollut. 2019;244:627–35.
185. Zhang C, Sui JH, Li J, Tang YL, Cai W. Efficient removal of heavy metal ions by thiol-functionalized superparamagnetic carbon nanotubes. Chem Eng J. 2012;203:369–76.
186. Huang L, He M, Chen B, Hu B. Mercapto-functionalized magnetic Zr-MOF via solvent-assisted ligand exchange for Hg^{2+} removal from water. J Mater Chem A. 2016;4:5159–66.
187. Liang L, Chen Q, Jiang F, Yuan D, Qian J, Lv G, Hong M. In situ large-scale construction of sulfur-functionalized metal–organic frameworks for efficient Hg(II) removal from water. J Mater Chem A. 2016;4:15370–4.
188. Saman N, Johari K, Mat H. Adsorption characteristics of sulfur-functionalized silica microspheres for Hg(II) removal from aqueous solutions. Ind Eng Chem Res. 2014;53:1225–33.
189. Saman N, Johari K, Mat H. Synthesis and characterization of sulfur-functionalized silica materials as adsorbents for mercury removal from aqueous solutions. Microporous Mesoporous Mater. 2014;194:38–45.
190. Qu J, Meng X, Jiang X, You H, Wang P, Ye X. Enhanced Cd(II) removal from water using sulfur-functionalized rice husk: characterization, adsorption performance, and mechanism. J Clean Prod. 2018;183:880–6.
191. Fan HT, Wu JB, Fan XL, Zhang DS, Su ZJ, Yan F, Sun T. Removal of Cd(II) and Pb(II) from aqueous solution using sulfur-functionalized silica prepared by a hydrothermal-assisted grafting method. Chem Eng J. 2012;198:355–63.
192. Zhang L, Zhang J, Li X, Wang C, Yu A, Zhang S, Cui Y. Adsorption behavior and mechanism of Hg(II) on a porous core–shell copper hydroxy sulfate@MOF composite. Appl Surf Sci. 2021;538:148054.
193. Ahmed MMM, Liao CH, Venkatesan S, Liu YT, Osman AI. Sulfur-functionalized sawdust biochar for enhanced cadmium adsorption and environmental remediation: a multidisciplinary approach and density functional theory insights. J Environ Manage. 2025;373:123586.
194. Singha Deb AK, Dhume N, Dasgupta K, Ali SM, Shenoy KT, Mohan S. Sulphur ligand functionalized carbon nanotubes for removal of mercury from wastewater—experimental and density functional theoretical study. Sep Sci Technol. 2019;54:1573–87.
195. Yang K, Wang Y, Wang D, Zhang Z, Gu P, Ren X, Miao H. Efficient removal of aqueous Cr(VI) using sulfur-modified biochar derived from anaerobic digestate: synergistic mechanism for reduction and sorption. Environ Sci Water Res Technol. 2025;11:2035–50.
196. Liu Q, Zhang H, Chen Y, Zhao X. Thiol-modified biochar with sulfur-containing functional groups for efficient mercury(II) removal from aqueous solutions. Sci Rep. 2025;15:26841.
197. Fang R, Lu C, Zhong Y, Xiao Z, Liang C, Huang H, Zhang W. Puffed rice carbon with coupled sulfur and metal iron for high-efficiency mercury removal in aqueous solution. Environ Sci Technol. 2020;54:2539–47.
198. Alhumaimess MS. Sulfhydryl functionalized activated carbon for Pb(II) ions removal: kinetics, isotherms, and mechanism. Sep Sci Technol. 2020;55:1303–16.
199. Li GP, Zhang K, Zhang PF, Liu WN, Tong WQ, Hou L, Wang YY. Thiol-functionalized pores via post-synthesis modification in a metal–organic framework with selective removal of Hg(II) in water. Inorg Chem. 2019;58:3409–15.
200. Singh N, Srivastava I, Dwivedi J, Sankararamakrishnan N. Ultrafast removal of Ppb levels of Hg(II) and volatile Hg(0) using post-modified metal organic framework. Chemosphere. 2021;270:129490.
201. Huang L, Shuai Q. Facile approach to prepare sulfur-functionalized magnetic amide-linked organic polymers for enhanced Hg(II) removal from water. ACS Sustain Chem Eng. 2019;7:9957–65.
202. Keshtkar AR, Moosavian MA, Sohbatzadeh H, Mofras M. La(III) and Ce(III) biosorption on sulfur functionalized marine brown algae *Cystoseira indica* by xanthation method: response surface methodology, isotherm, and kinetic study. Groundw Sustain Dev. 2019;8:144–55.
203. Huang L, Shen R, Liu R, Shuai Q. Thiol-functionalized magnetic covalent organic frameworks by a cutting strategy for efficient removal of Hg^{2+} from water. J Hazard Mater. 2020;392:122320.
204. Pirveysian M, Ghiaci M. Synthesis and characterization of sulfur functionalized graphene oxide nanosheets as efficient sorbent for removal of Pb^{2+}, Cd^{2+}, Ni^{2+}, and Zn^{2+} ions from aqueous solution: a combined thermodynamic and kinetic study. Appl Surf Sci. 2018;428:98–109.
205. Feng W, Borguet E, Vidic RD. Sulfurization of a carbon surface for vapor phase mercury removal–II: sulfur forms and mercury uptake. Carbon. 2006;44:2998–3004.

206. Xia Z, Baird L, Zimmerman N, Yeager M. Heavy metal ion removal by thiol functionalized aluminum oxide hydroxide nanowhiskers. Appl Surf Sci. 2017;416:565–73.
207. Choi J, Lee KM, Wycisk R, Pintauro PN, Mather PT. Nanofiber network ion-exchange membranes. Macromolecules. 2008;41:4569–72.
208. Pan F, Tong C, Wang Z, Xu F, Wang X, Weng B, Zhu R. Novel sulfhydryl functionalized covalent organic frameworks for ultra-trace Hg^{2+} removal from aqueous solution. J Mater Sci Technol. 2021;93:89–95.
209. Zubrik A, Matik M, Lovás M, Danková Z, Kaňuchová M, Hredzák S, Šepelák V. Mechanochemically synthesised coal-based magnetic carbon composites for removing As(V) and Cd(II) from aqueous solutions. Nanomaterials. 2019;9:100.
210. Kumar S, Loganathan VA, Gupta RB, Barnett MO. An assessment of U(VI) removal from groundwater using biochar produced from hydrothermal carbonization. J Environ Manag. 2011;92:2504–12.
211. Cui Y, Masud A, Aich N, Atkinson JD. Phenol and Cr(VI) removal using materials derived from harmful algal bloom biomass: characterization and performance assessment for a biosorbent, a porous carbon, and Fe/C composites. J Hazard Mater. 2019;368:477–86.
212. Sujatha S, Venkatesan G, Sivarethinamohan R. Optimization of lead removal in exhausting Manilkara Zapota based activated carbon: application of response surface methodology. Environ Technol. 2020;41:2478–93.
213. Chen Q, Zheng J, Wen L, Yang C, Zhang L. A multi-functional-group modified cellulose for enhanced heavy metal cadmium adsorption: performance and quantum chemical mechanism. Chemosphere. 2019;224:509–18.
214. Imamoglu M, Ozturk A, Aydın Ş, Manzak A, Gündoğdu A, Duran C. Adsorption of Cu(II) ions from aqueous solution by hazelnut husk activated carbon prepared with potassium acetate. J Dis Sci Technol. 2018;39:1144–8.
215. Elmorsi RR, El-Wakeel ST, Shehab El-Dein WA, Lotfy HR, Rashwan WE, Nagah M, Abou-El-Sherbini KS. Adsorption of methylene blue and Pb^{2+} by using acid-activated posidonia oceanica waste. Sci Rep. 2019;9:3356.
216. Wu W, Yang Y, Zhou H, Ye T, Huang Z, Liu R, Kuang Y. Highly efficient removal of Cu(II) from aqueous solution by using graphene oxide. Water Air Soil Pollut. 2013;224:1–8.
217. Ibrahim WM, Hassan AF, Azab YA. Biosorption of toxic heavy metals from aqueous solution by Ulva lactuca activated carbon. Egypt J Basic Appl Sci. 2016;3:241–9.
218. Lei Y, et al. Three-dimensional magnetic graphene oxide foam/Fe_3O_4 nanocomposite as an efficient absorbent for Cr(VI) removal. J Mater Sci. 2014;49:4236–45.

Publisher's note